

SIMULATION AND INTERPRETATION OF BOREHOLE GEOPHYSICAL MEASUREMENTS USING *hp* FINITE ELEMENTS

***hp*-FEM team: D. Pardo, M. J. Nam , L. Demkowicz,
C. Torres-Verdín, V. M. Calo,
M. Paszynski, and P. J. Matuszyk**

8th Annual Formation Evaluation
Research Consortium Meeting
August 14-15, 2008



Overview

1. Main Lines of Research and Applications (D. Pardo)

- Previous work
- Main features of our technology

2. Application 1: Tri-Axial Induction Instruments (M. J. Nam)

3. Application 2: Dual-Laterolog Instruments (M. J. Nam)

4. Multi-Physics Inversion (D. Pardo)

5. Sonic Instruments (L. Demkowicz)



Previous Work

Type of Problems We Can Solve with our *hp*-FEM software

Applications	Borehole Measurements	Marine Controlled Source EM	
Spatial Dimensions	2D	3D	
Well Type	Vertical Well	Deviated Well	Eccentered Tool
Logging Instruments	LWD/MWD	Normal/Laterolog	Dual-Laterolog
	Induction	Dielectric Instruments	Cross-Well
Frequency	0 ~ 10 GHz		
Materials	Isotropic	Anisotropic	
Physical Devices	Magnetic Buffers	Insulators	Casing
	Casing Imperfections	Displacement Currents	Combination of All
Sources	Finite Size Antennas	Dipoles in Any Direction	Solenoidal Antennas
	Toroidal Antennas	Electrodes	Combination of All
Invasion	Water	Oil	etc.

MOST (OIL-INDUSTRY) GEOPHYSICAL PROBLEMS

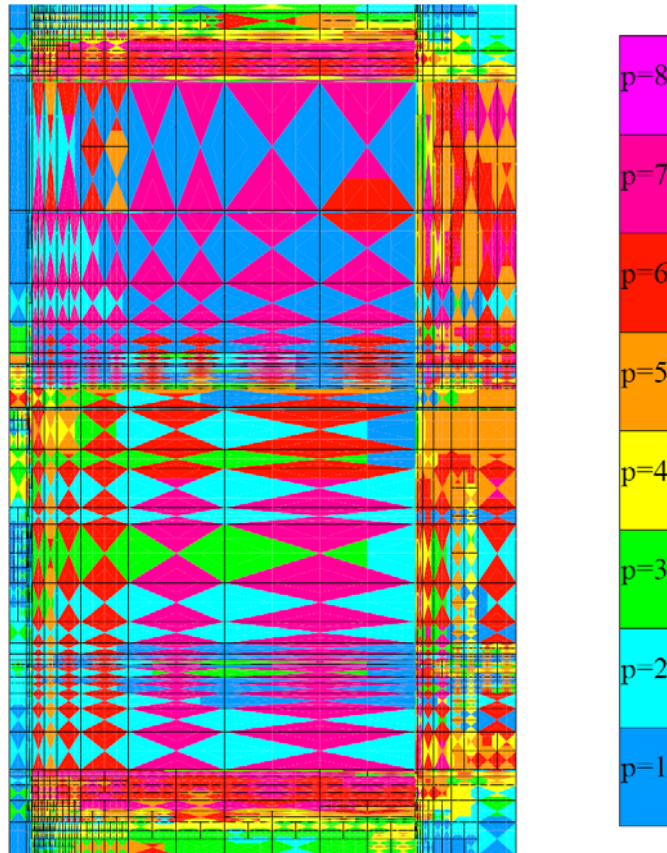


Main Features of Our Technology

- 1. Self-Adaptive Goal-Oriented *hp*-Refinements**
- 2. Fourier Finite-Element Method**
- 3. Parallel Implementation**



Self-Adaptive Goal-Oriented hp -FEM



We vary locally the element size h and the polynomial order of approximation p throughout the grid.

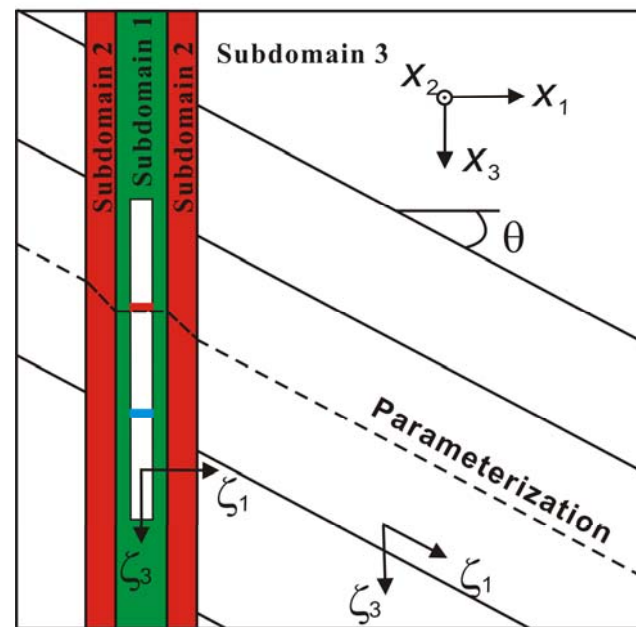
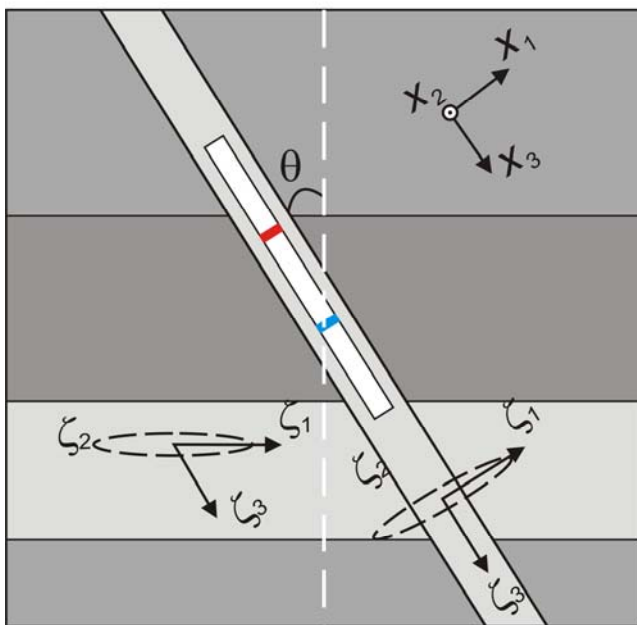
Optimal grids are **automatically generated** by the hp -algorithm.

The self-adaptive goal-oriented hp -FEM provides **exponential convergence** rates in terms of the CPU time vs. the error in a user prescribed quantity of Interest.

3D Deviated Well

Cartesian system of coordinates: (x_1, x_2, x_3)

New non-orthogonal system of coordinates: $(\zeta_1, \zeta_2, \zeta_3)$



Subdomain 1

$$\begin{cases} x_1 = \zeta_1 \cos \zeta_2 \\ x_2 = \zeta_1 \sin \zeta_2 \\ x_3 = \zeta_3 \end{cases}$$

Subdomain 2

$$\begin{cases} x_1 = \zeta_1 \cos \zeta_2 \\ x_2 = \zeta_1 \sin \zeta_2 \\ x_3 = \zeta_3 + \tan \theta \frac{\zeta_1 - \rho_1}{\rho_2 - \rho_1} \rho_2 \cos \zeta_2 \end{cases}$$

Subdomain 3

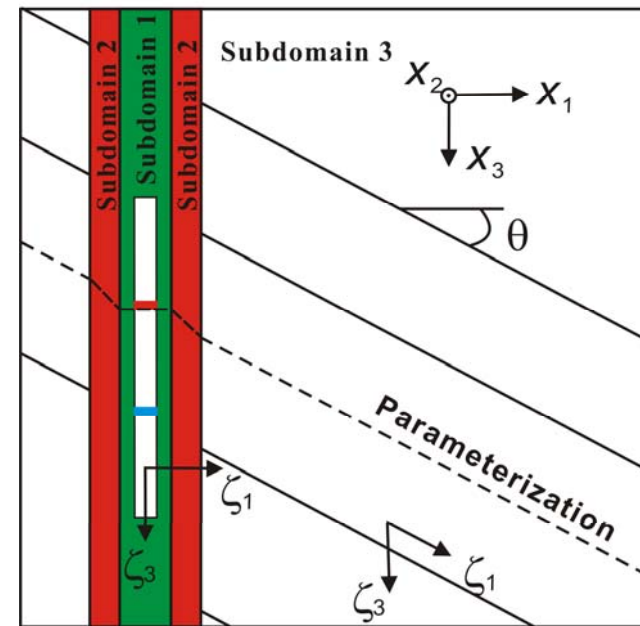
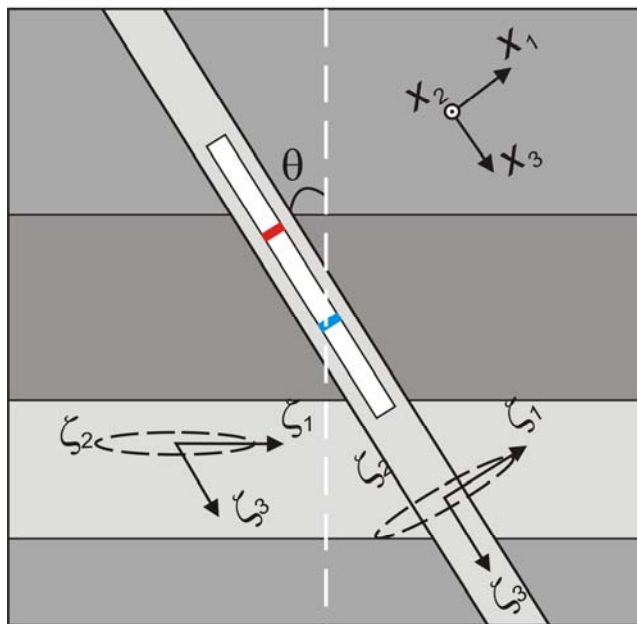
$$\begin{cases} x_1 = \zeta_1 \cos \zeta_2 \\ x_2 = \zeta_1 \sin \zeta_2 \\ x_3 = \zeta_3 + \zeta_1 \tan \theta \cos \zeta_2 \end{cases}$$



3D Deviated Well

Cartesian system of coordinates: (x_1, x_2, x_3)

New non-orthogonal system of coordinates: $(\zeta_1, \zeta_2, \zeta_3)$



Constant material coefficients in the quasi-azimuthal direction ζ_2
in the new non-orthogonal system of coordinates!!!!



3D Deviated Well

*For each Fourier mode, we obtain a 2D problem. Each 2D problem couples with **up to five different 2D problems** corresponding to different Fourier modes, therefore, constituting the resulting 3D problem.*

When we use 9 Fourier Modes for the Solution:

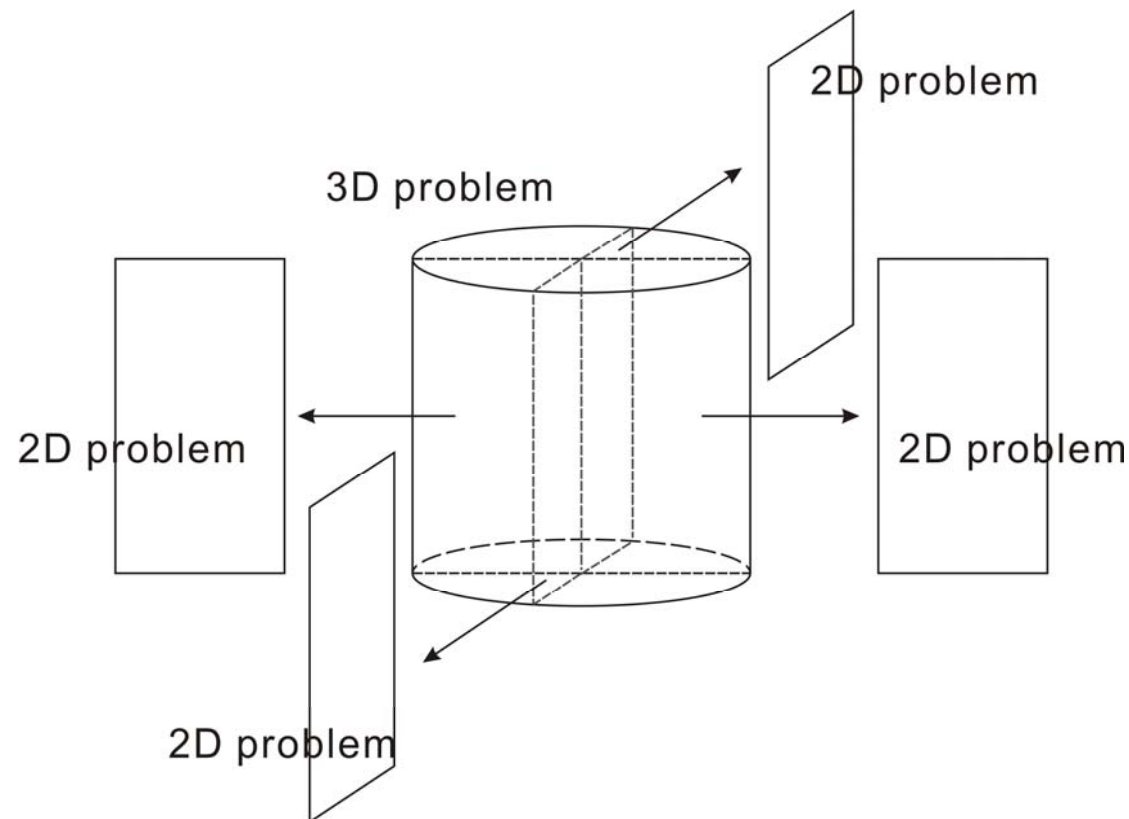
$$\begin{bmatrix}
 A_{1,1} & A_{1,2} & A_{1,3} & 0 & 0 & 0 & 0 & 0 & 0 \\
 A_{2,1} & A_{2,2} & A_{2,3} & A_{2,4} & 0 & 0 & 0 & 0 & 0 \\
 A_{3,1} & A_{3,2} & A_{3,3} & A_{3,4} & A_{3,5} & 0 & 0 & 0 & 0 \\
 0 & A_{4,2} & A_{4,3} & A_{4,4} & A_{4,5} & A_{4,6} & 0 & 0 & 0 \\
 0 & 0 & A_{5,3} & A_{5,4} & A_{5,5} & A_{5,6} & A_{5,7} & 0 & 0 \\
 0 & 0 & 0 & A_{6,4} & A_{6,5} & A_{6,6} & A_{6,7} & A_{6,8} & 0 \\
 0 & 0 & 0 & 0 & A_{7,5} & A_{7,6} & A_{7,7} & A_{7,8} & A_{7,9} \\
 0 & 0 & 0 & 0 & 0 & A_{8,6} & A_{8,7} & A_{8,8} & A_{8,9} \\
 0 & 0 & 0 & 0 & 0 & 0 & A_{9,7} & A_{9,8} & A_{9,9}
 \end{bmatrix}
 \begin{bmatrix}
 x_1 \\
 x_2 \\
 x_3 \\
 x_4 \\
 x_5 \\
 x_6 \\
 x_7 \\
 x_8 \\
 x_9
 \end{bmatrix}
 =
 \begin{bmatrix}
 b_1 \\
 b_2 \\
 b_3 \\
 b_4 \\
 b_5 \\
 b_6 \\
 b_7 \\
 b_8 \\
 b_9
 \end{bmatrix}$$

$A_{i,j}$: represents a full 2D problem for each Fourier basis function



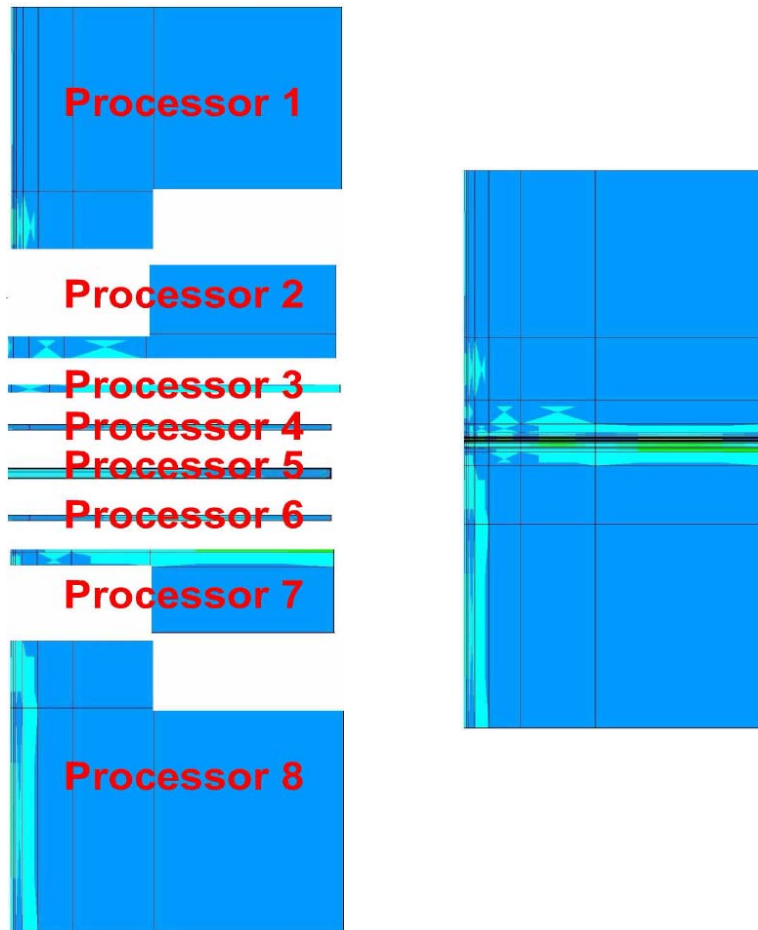
3D Deviated Well

*For each Fourier mode, we obtain a 2D problem. Each 2D problem couples with **up to five different 2D problems** corresponding to different Fourier modes, therefore, constituting the resulting 3D problem.*

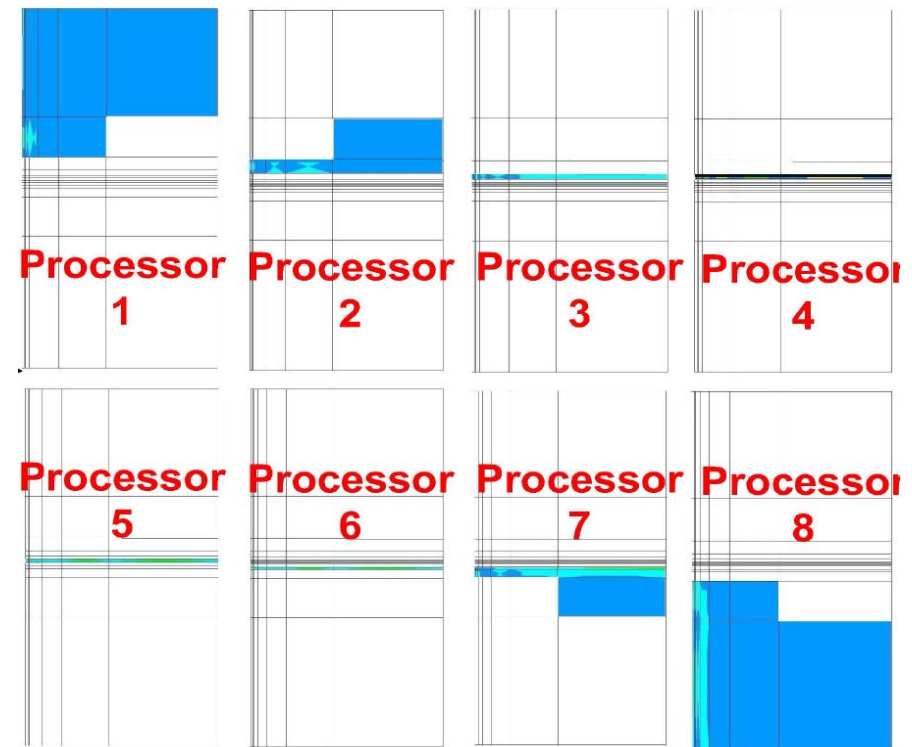



3D Parallelization Implementation

Distributed Domain Decomposition



Shared Domain Decomposition!!





SELF-ADAPTIVE *hp* FINITE-ELEMENT SIMULATION OF MULTI-COMPONENT INDUCTION MEASUREMENTS ACQUIRED IN DIPPING, INVADED, AND ANISOTROPIC FORMATIONS

M. J. Nam, D. Pardo, and C. Torres-Verdín,
The University of Texas at Austin

hp-FEM team: D. Pardo, M. J. Nam, L. Demkowicz, C. Torres-Verdín,
V. M. Calo, M. Paszynski, and P. J. Matuszlik

8th Annual Formation Evaluation
Research Consortium Meeting
August 14-15, 2008



Overview

1. Main Lines of Research and Applications (D. Pardo)

- Previous work
- Main features of our technology

2. Application 1: Tri-Axial Induction Instruments (M. J. Nam)

3. Application 2: Dual-Laterolog Instruments (M. J. Nam)

4. Multi-Physics Inversion (D. Pardo)

5. Sonic Instruments (L. Demkowicz)

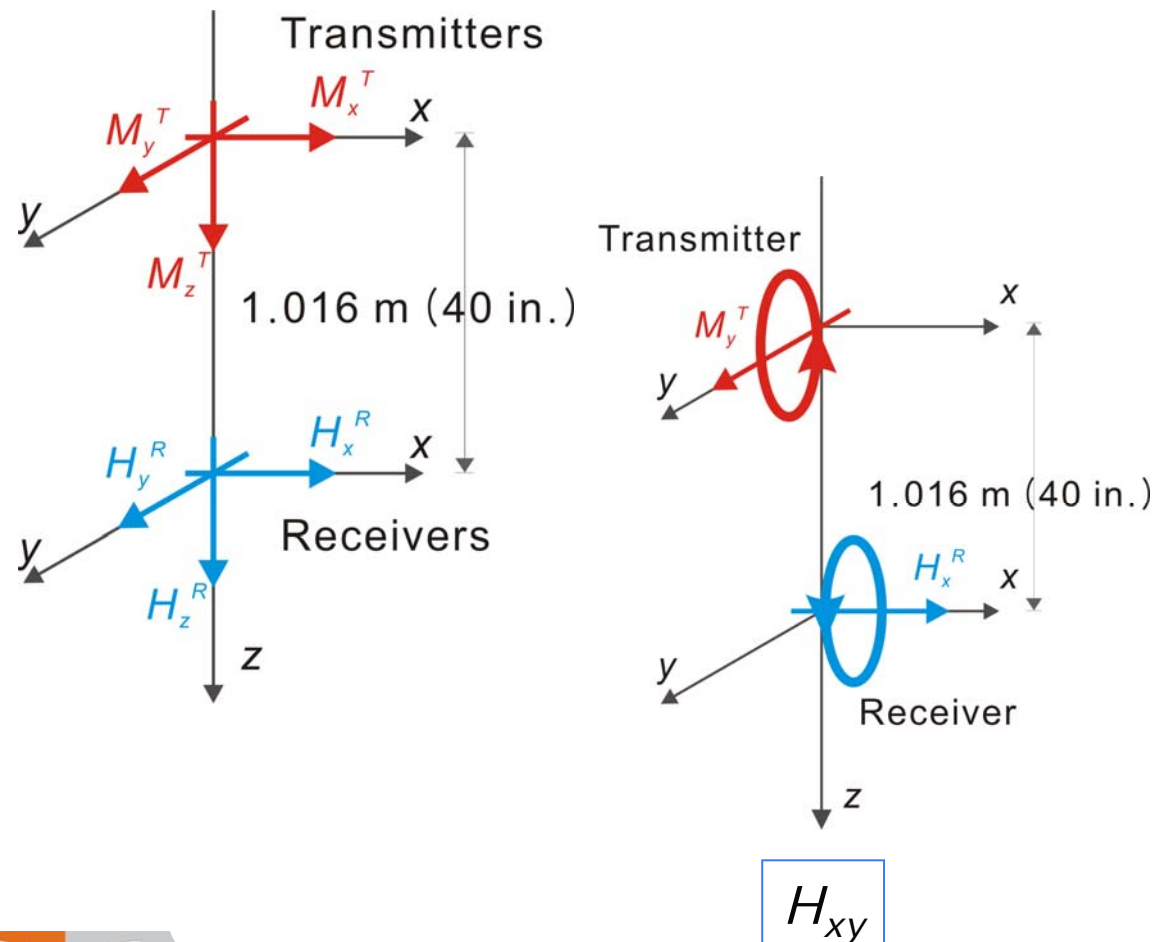


Outline

- **Introduction to Tri-Axial Induction**
- **Method**
- **Numerical Results:**
 - **Verification of 3D Method for Tri-Axial Induction Tool**
 - **Dipping, Invaded, Anisotropic Formations**
- **Conclusions**

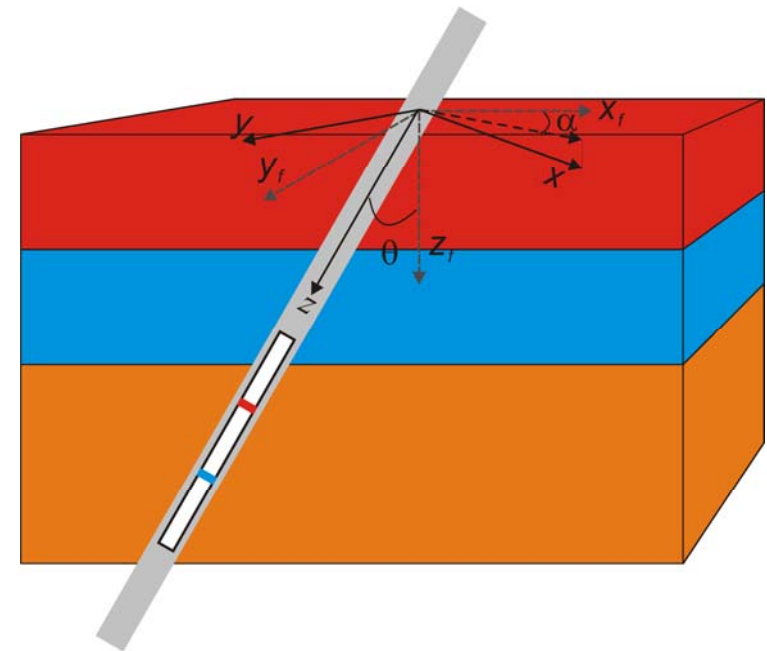


Tri-Axial Induction Tool



$L = 1.016 \text{ m (40 in.)}$

Operating frequency: 20 kHz



θ : dip angle

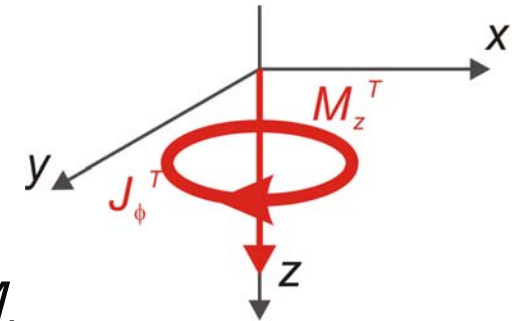
α : tool orientation angle



3D Source Implementation

1. Solenoidal Coil (J_ϕ) for M_z

→ becoming a 2D source in (ρ, ϕ, z)

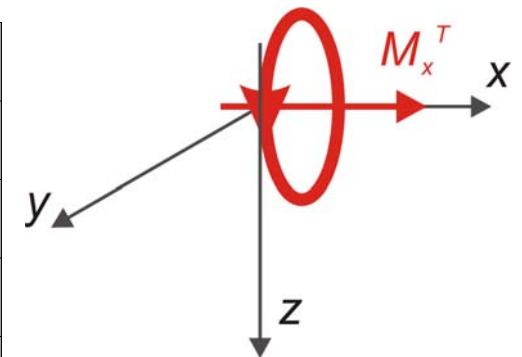
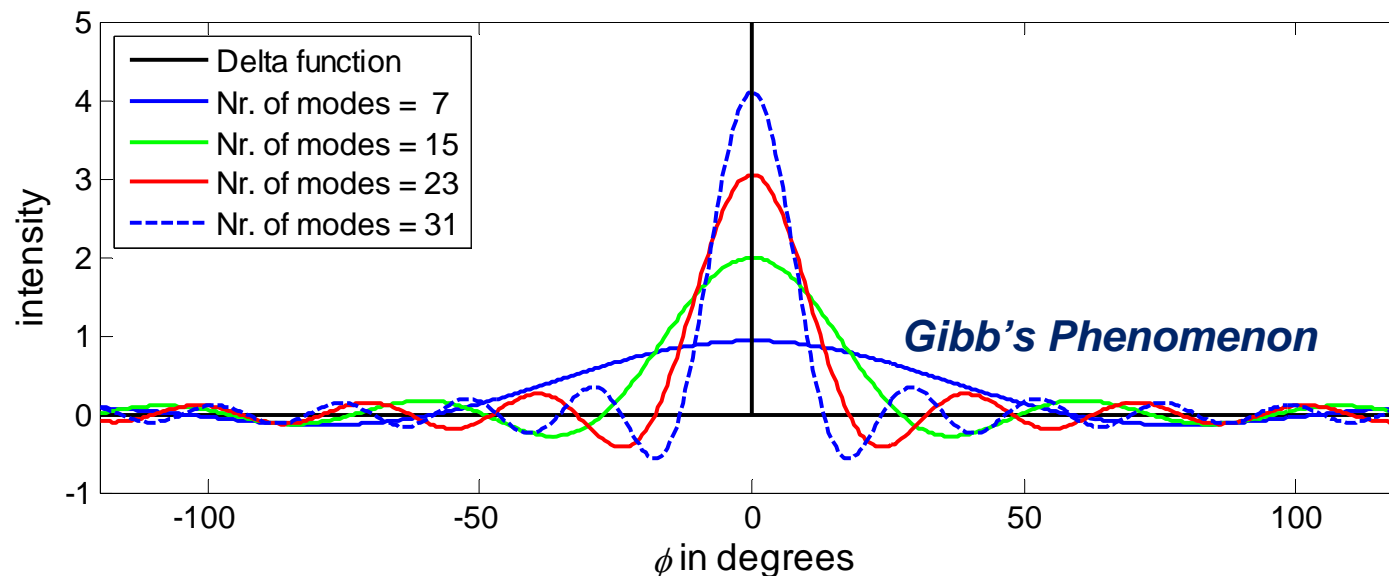


2. Delta Function for 3D source M_x or M_y

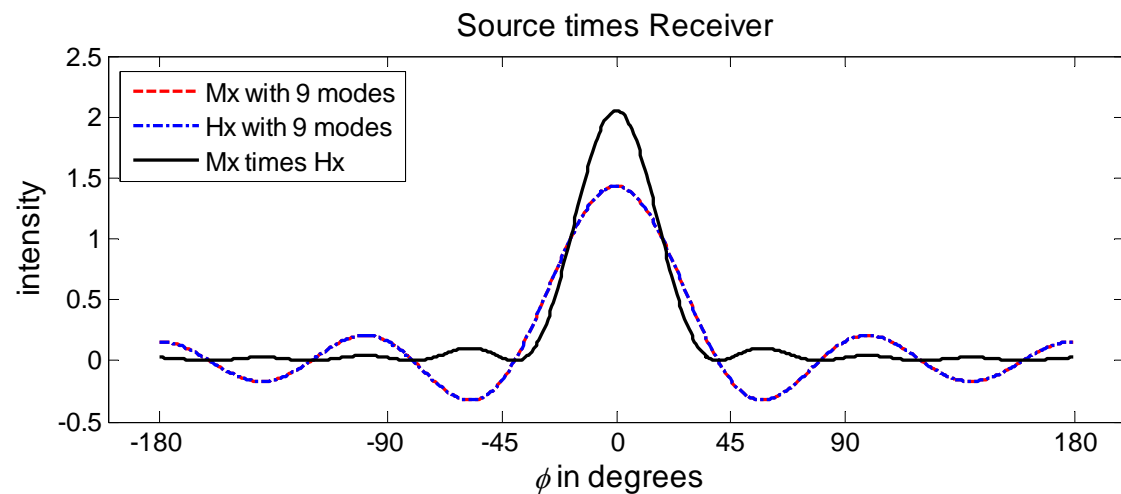
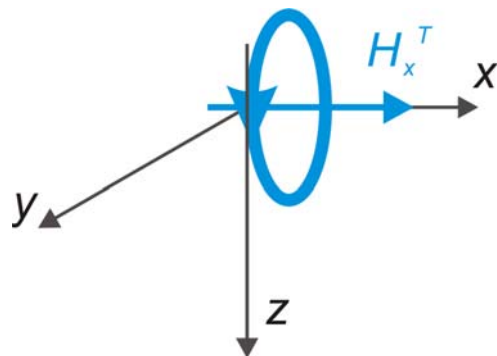
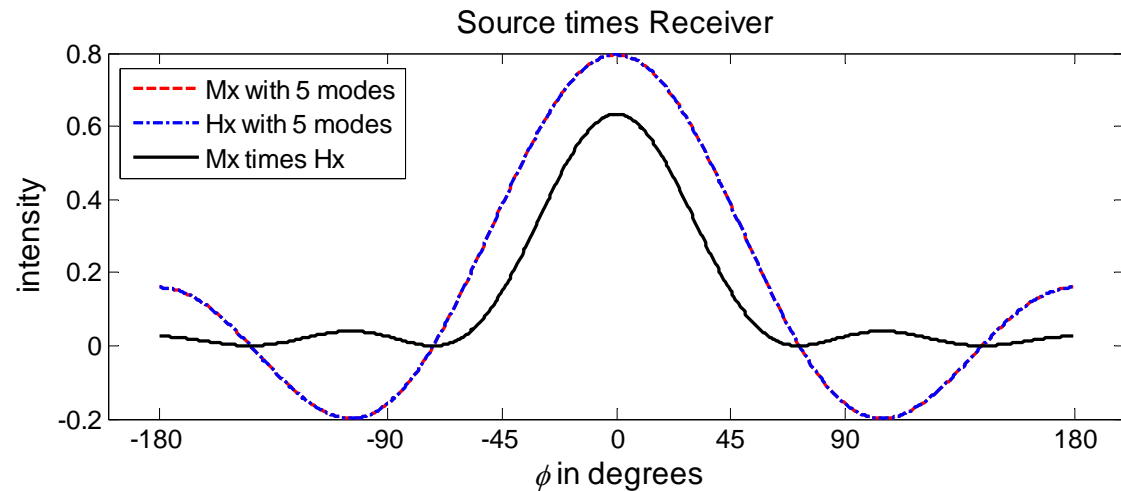
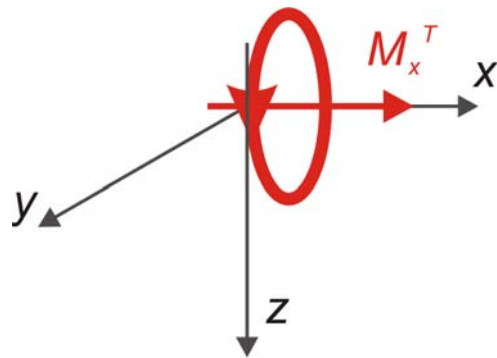
$$f(\phi) = \delta(\phi - \phi_0)$$

ϕ_0 : the position of the center of the peak
(0° for M_x ; 90° for M_y)

M_x : Delta function



3D Source and Receiver (Delta Functions)



***Coupling between source and receiver:
less Gibb's phenomenon***



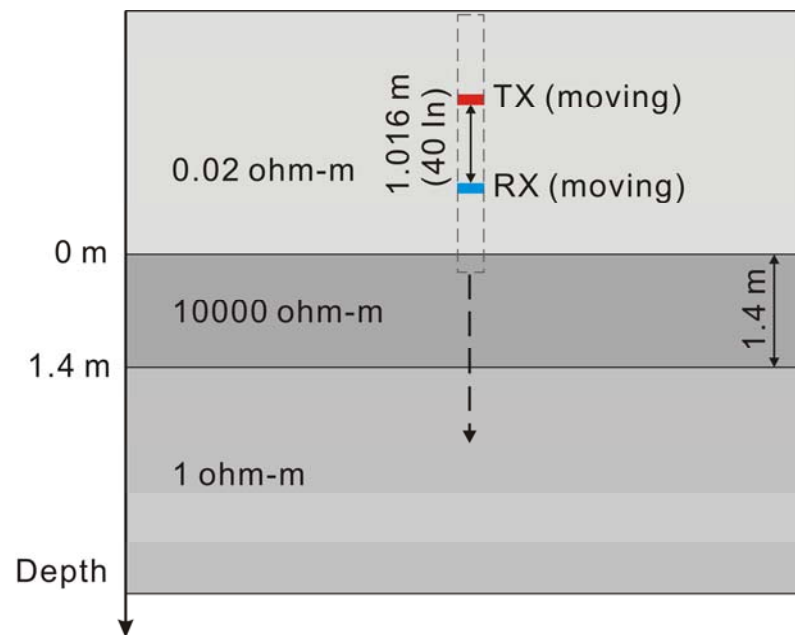
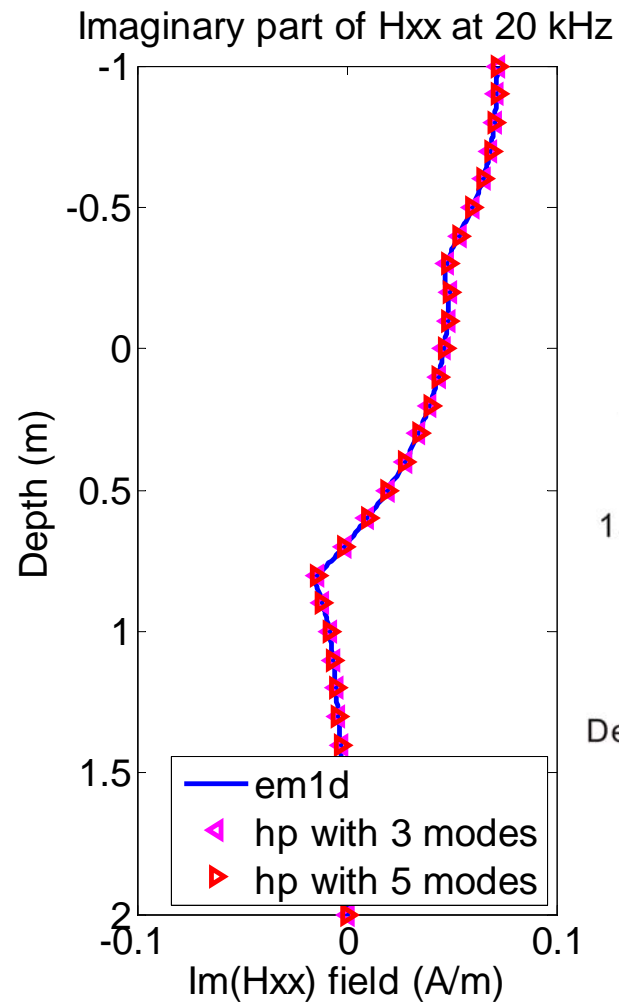
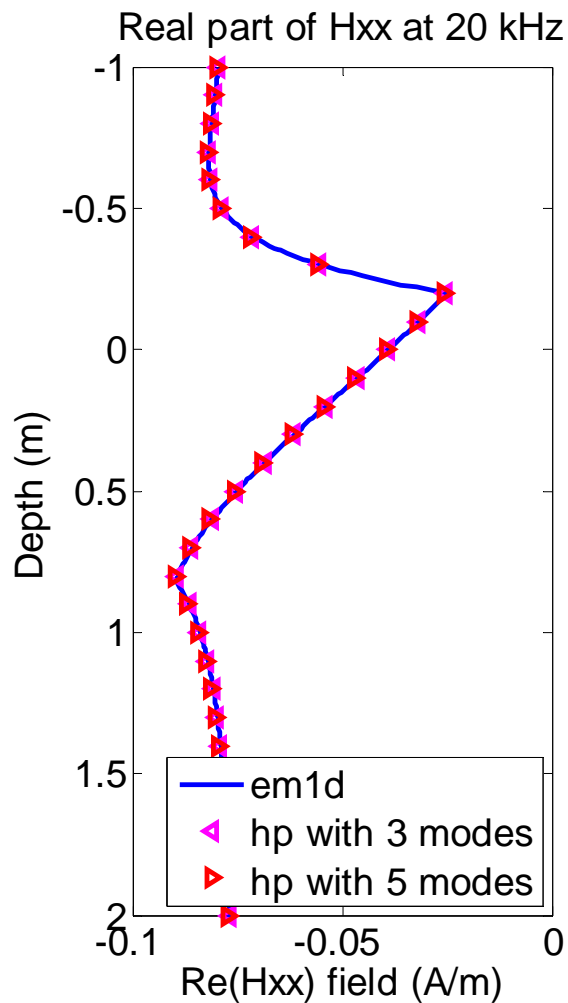
Method

Combination of:

- 1. A Self-Adaptive Goal-Oriented *hp*-FEM
for AC problems**
- 2. A Fourier Series Expansion
in a Non-Orthogonal System of Coordinates**
- 3. Parallel Implementation**



Verification of 2.5D Simulation ($H_{xx} = H_{yy}$)

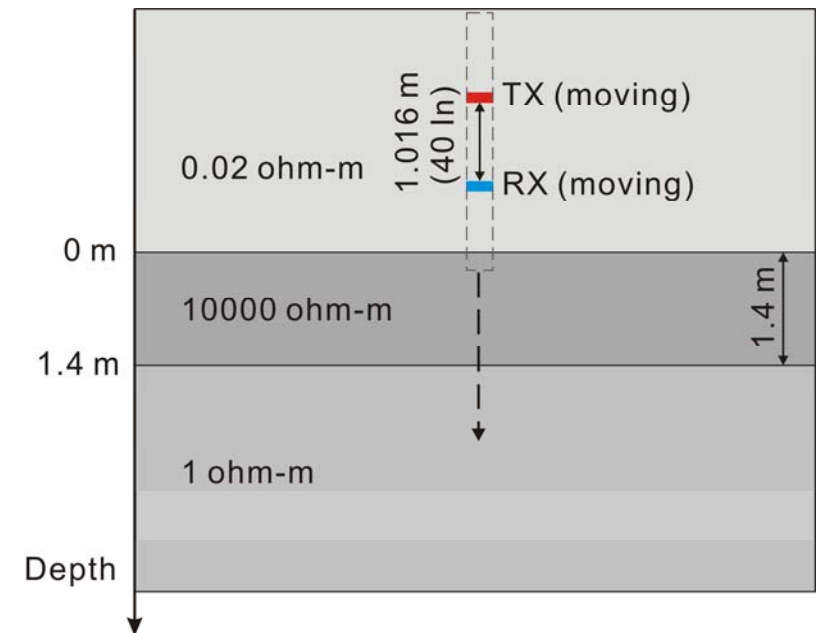
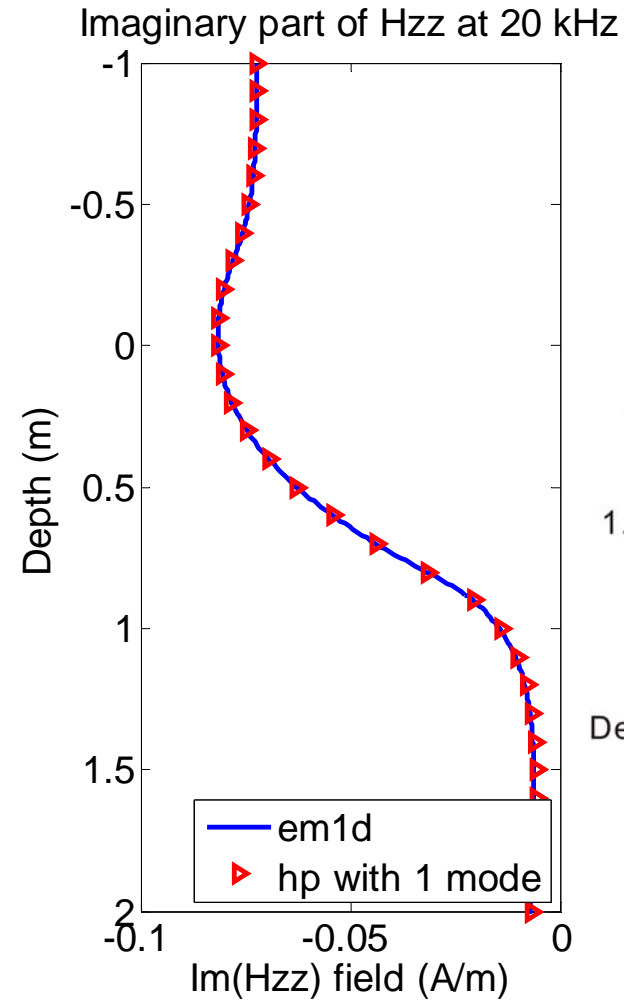
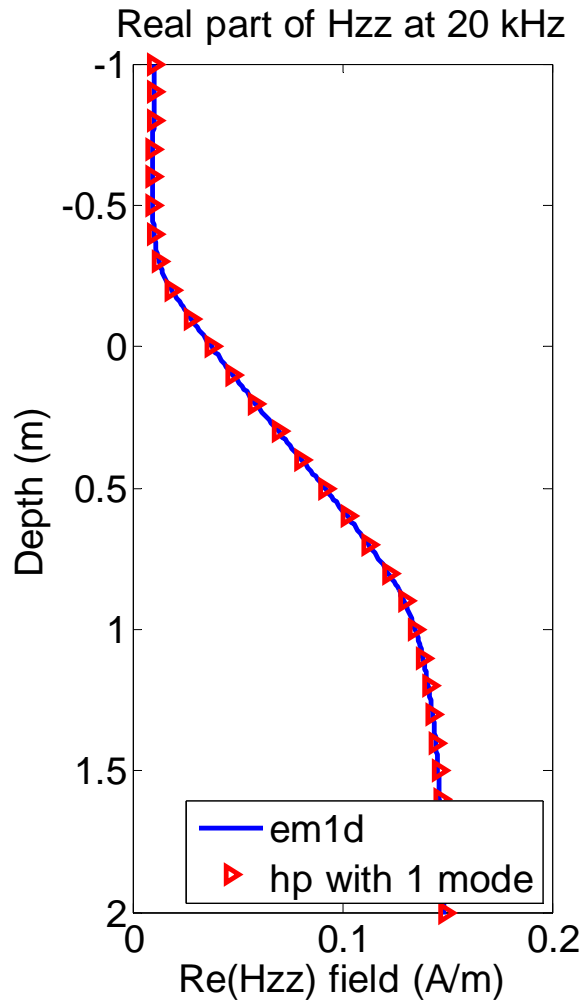


**Converged solutions
with 3 Fourier modes**

em1D: K. H. Lee 1984, pers. comm.



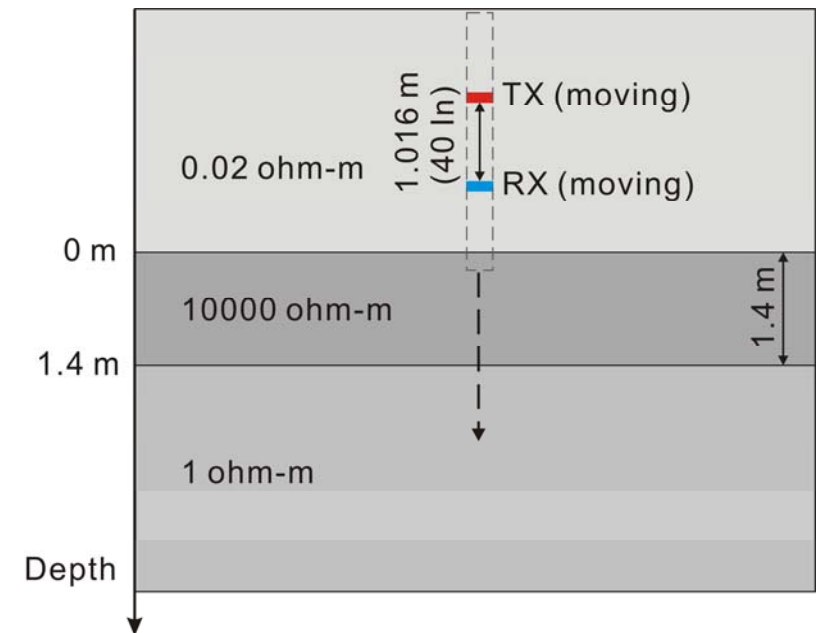
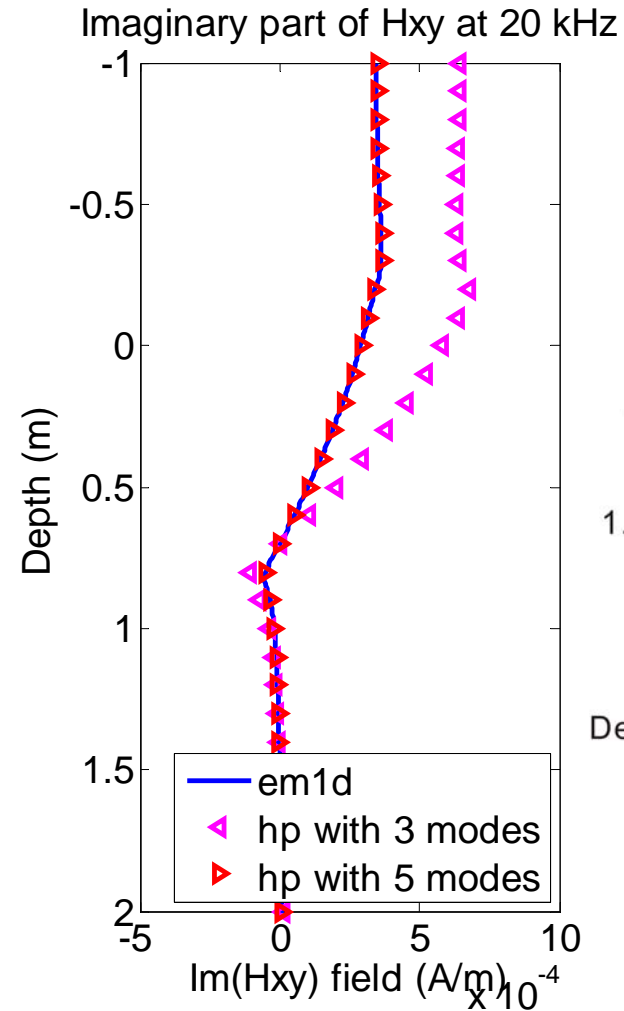
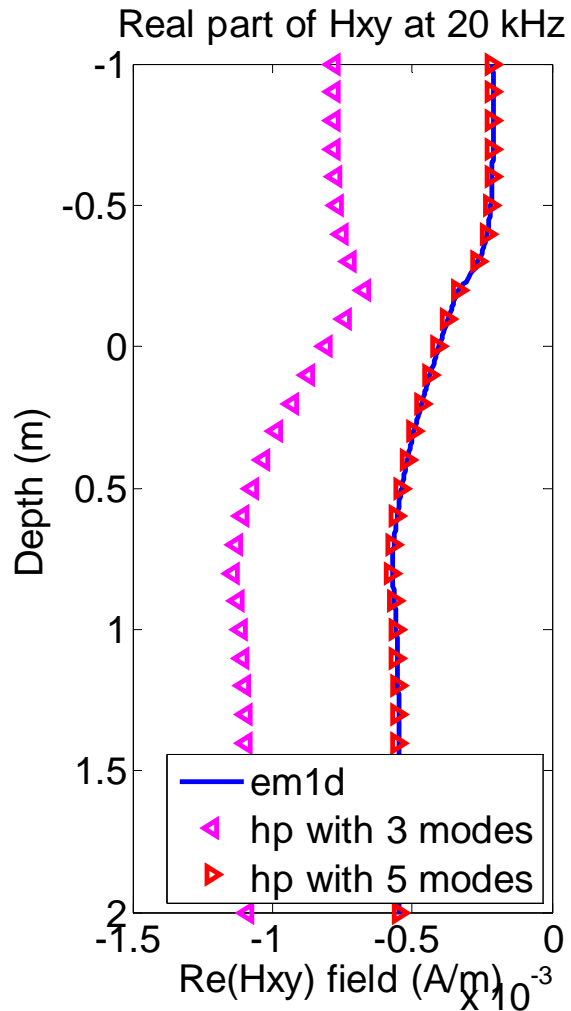
Verification of 2.5D Simulation (H_{zz})



The same solutions
with 1 Fourier mode



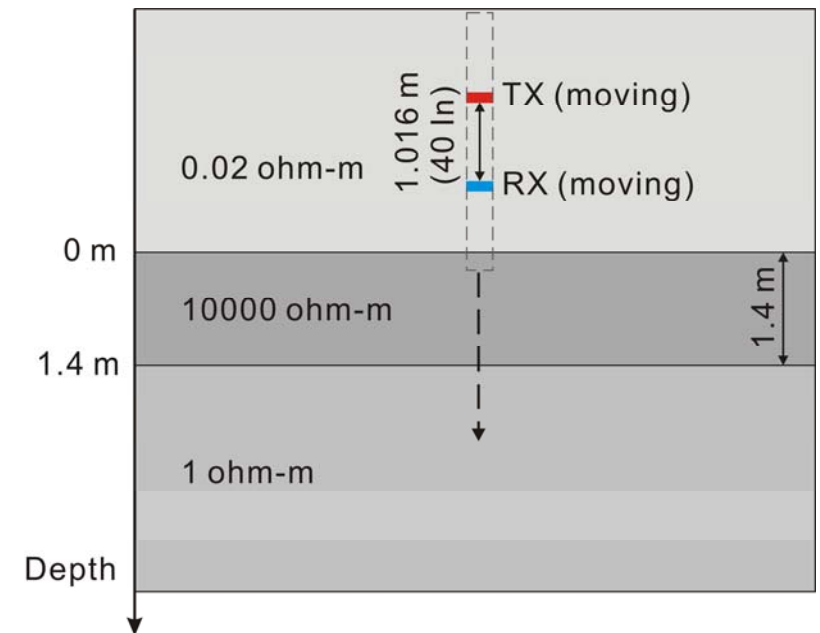
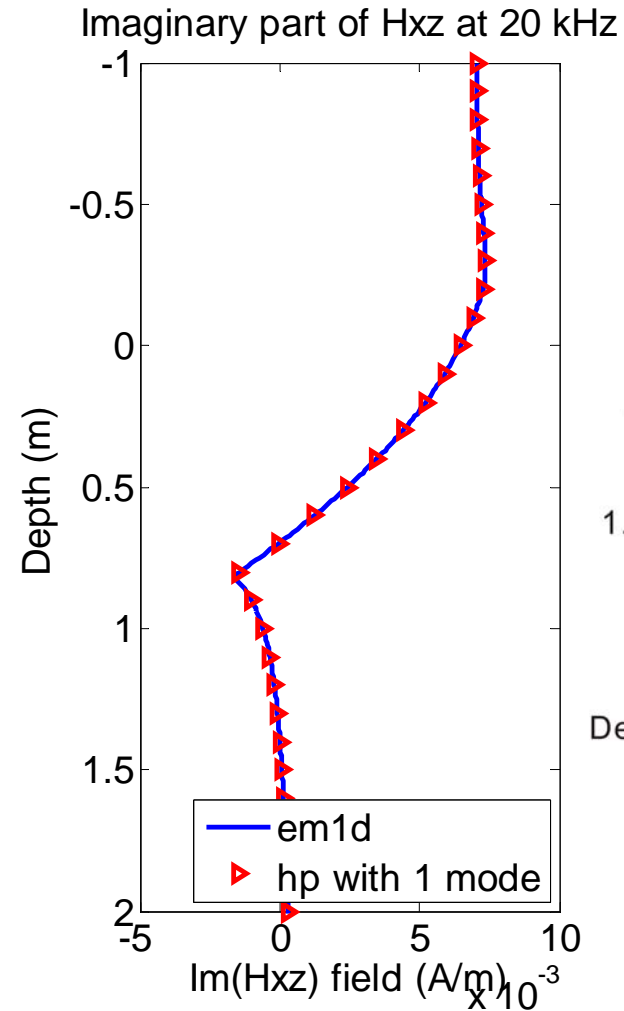
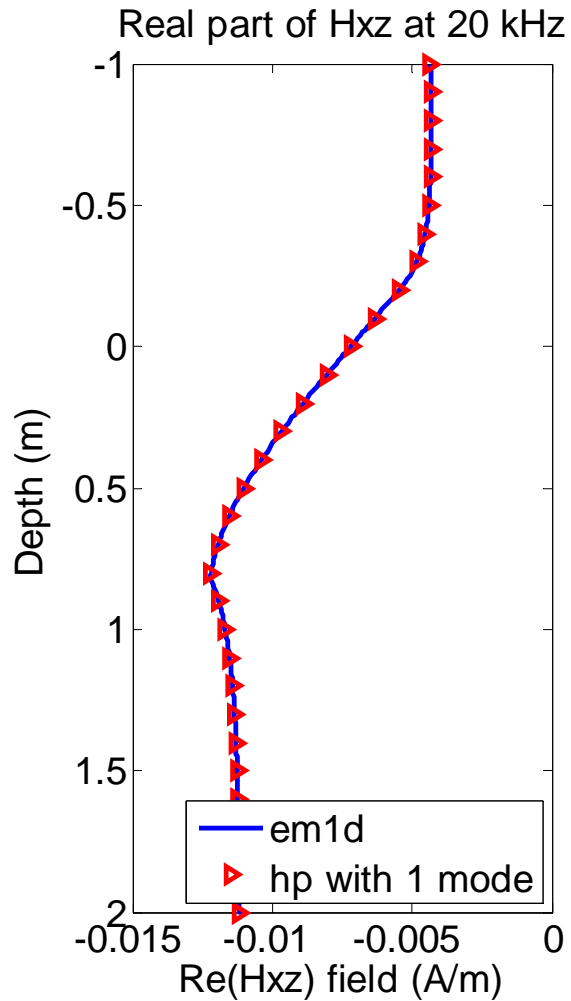
Verification of 2.5D Simulation ($H_{xy} = H_{yx}$)



**Converged solutions
with 5 Fourier modes**



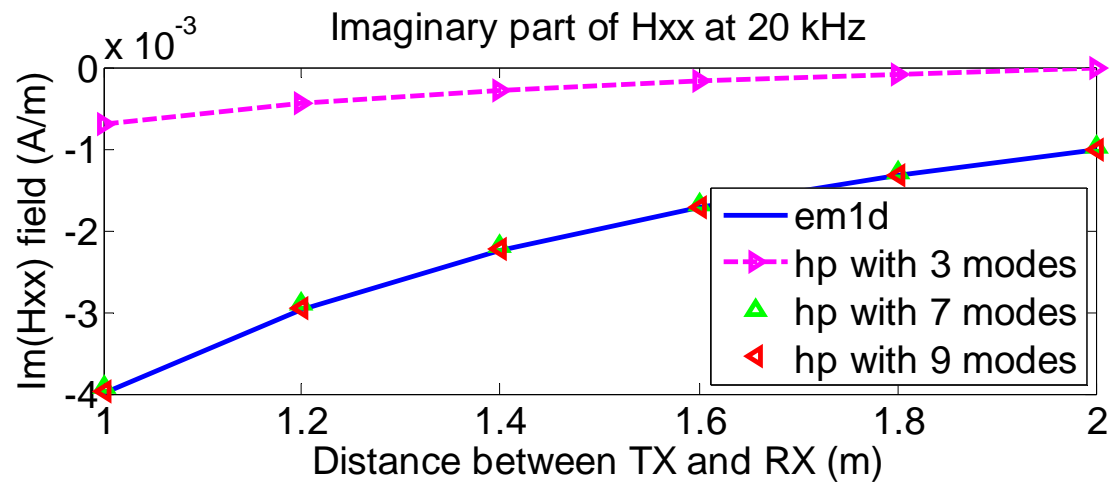
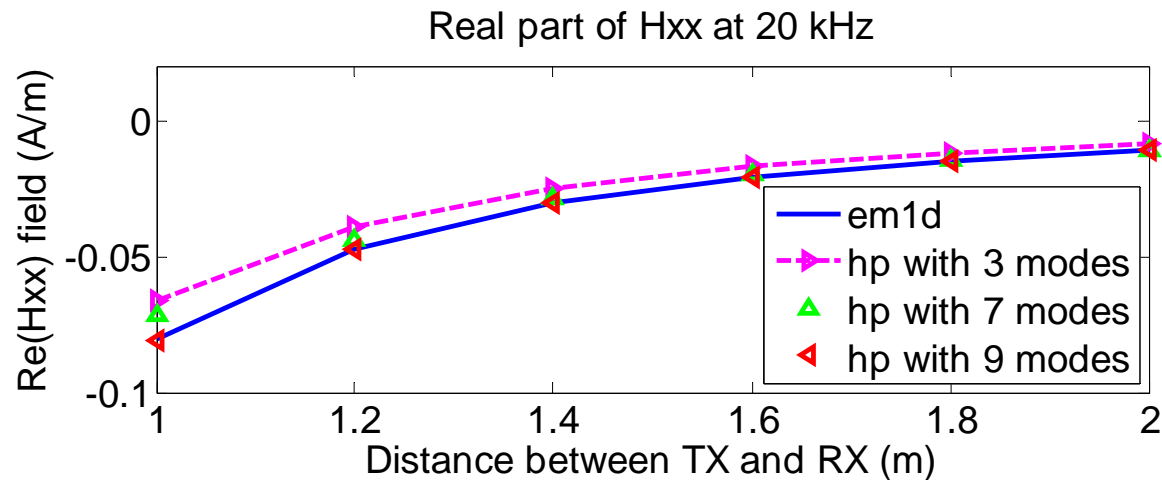
Verification of 2.5D Simulation ($H_{xz} = H_{zx}$)



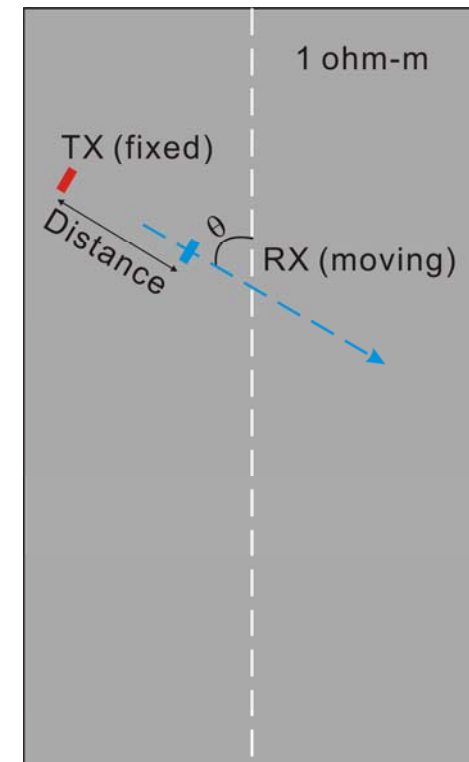
**The same solutions
with 1 Fourier mode**



Verification of 3D Simulation ($H_{xx} = H_{yy}$)



Dip angle: 60 degrees

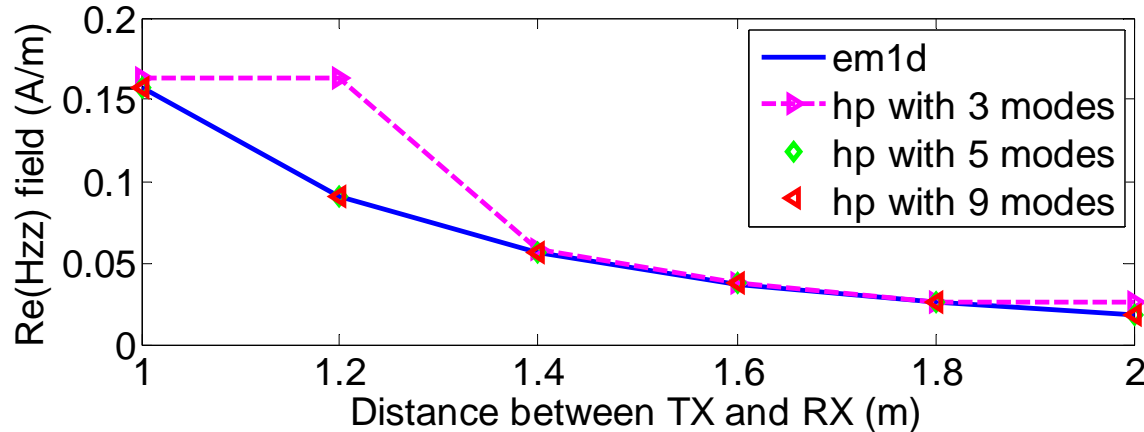


Converged solutions
with 9 Fourier mode

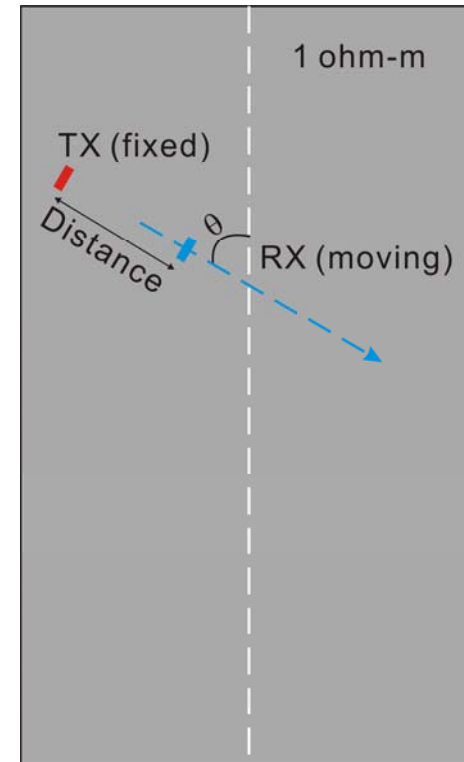


Verification of 3D Simulation (H_{zz})

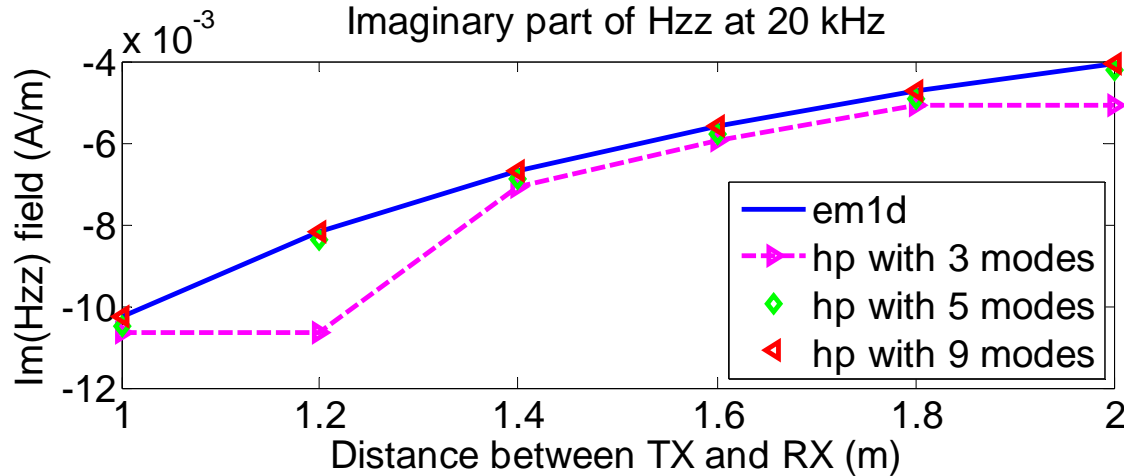
Real part of H_{zz} at 20 kHz



Dip angle: 60 degrees



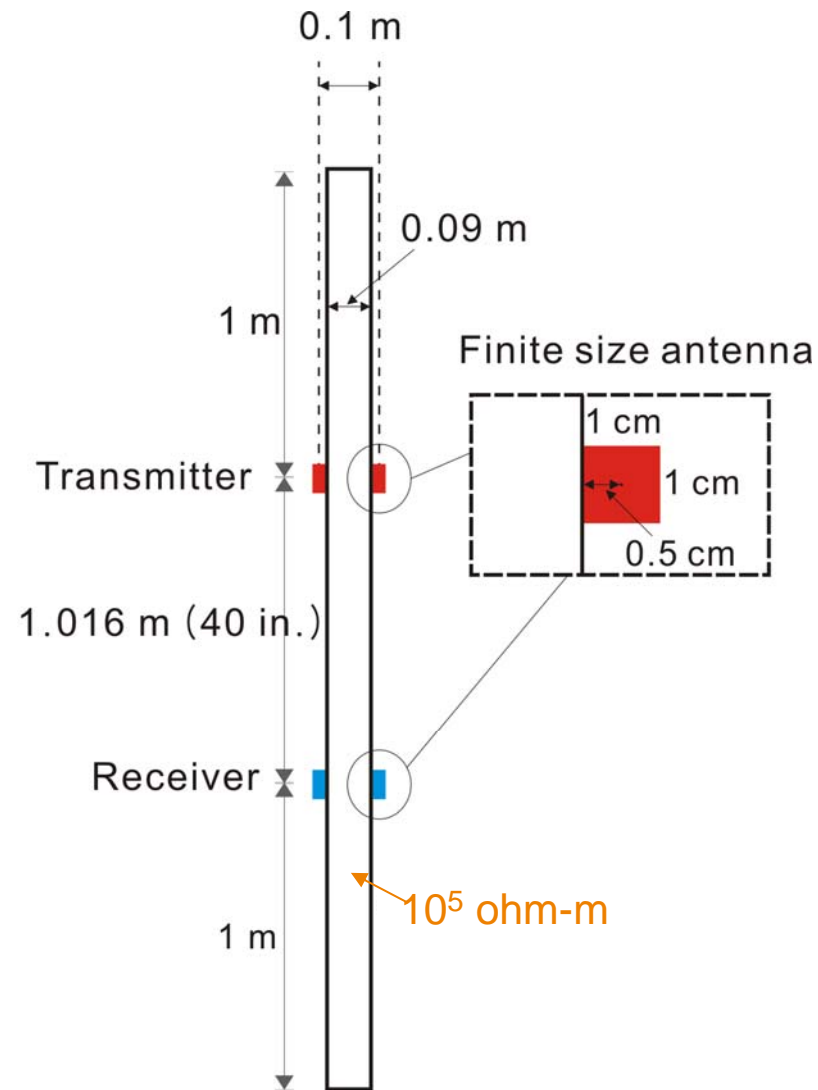
Imaginary part of H_{zz} at 20 kHz



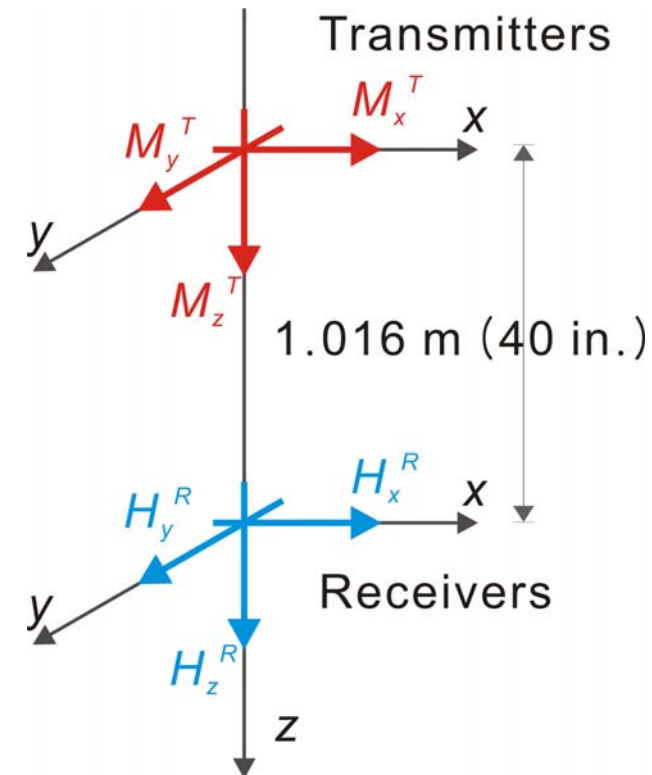
Converged solutions with 5 Fourier mode



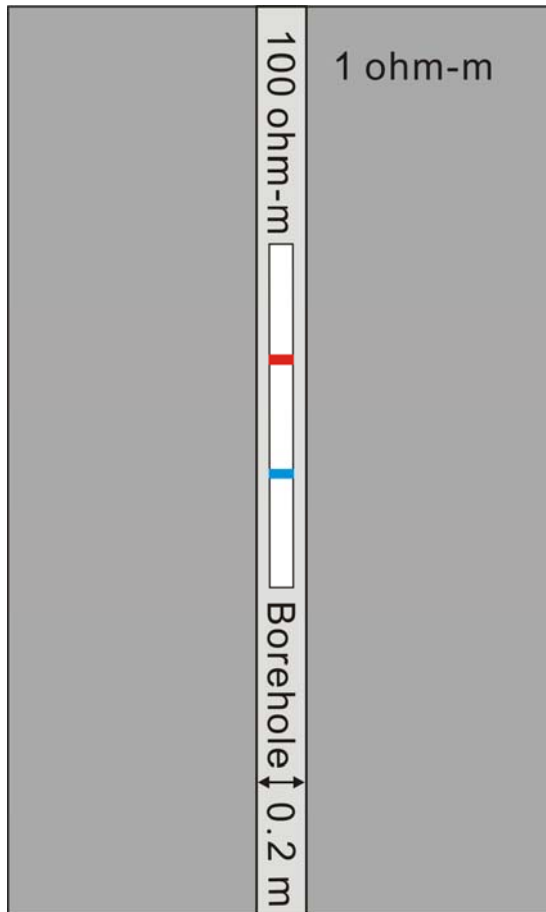
Description of the Tri-Axial Tool



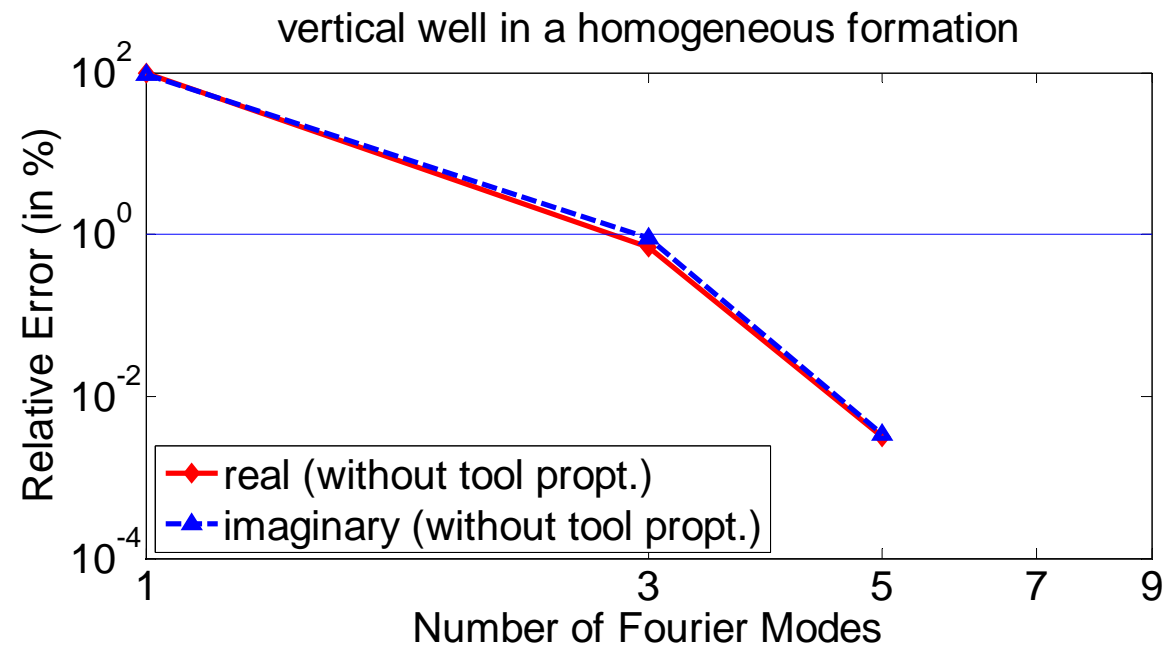
Operating frequency: 20 kHz



Verification of 2.5D Simulation (H_{xx})

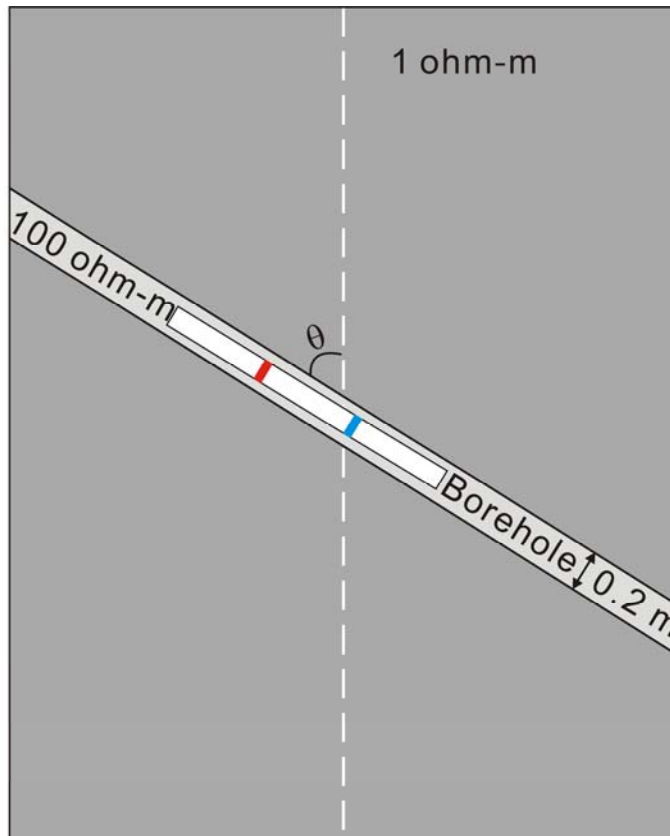


Relative errors of tri-axial induction solutions with respect to the solution with 9 Fourier modes

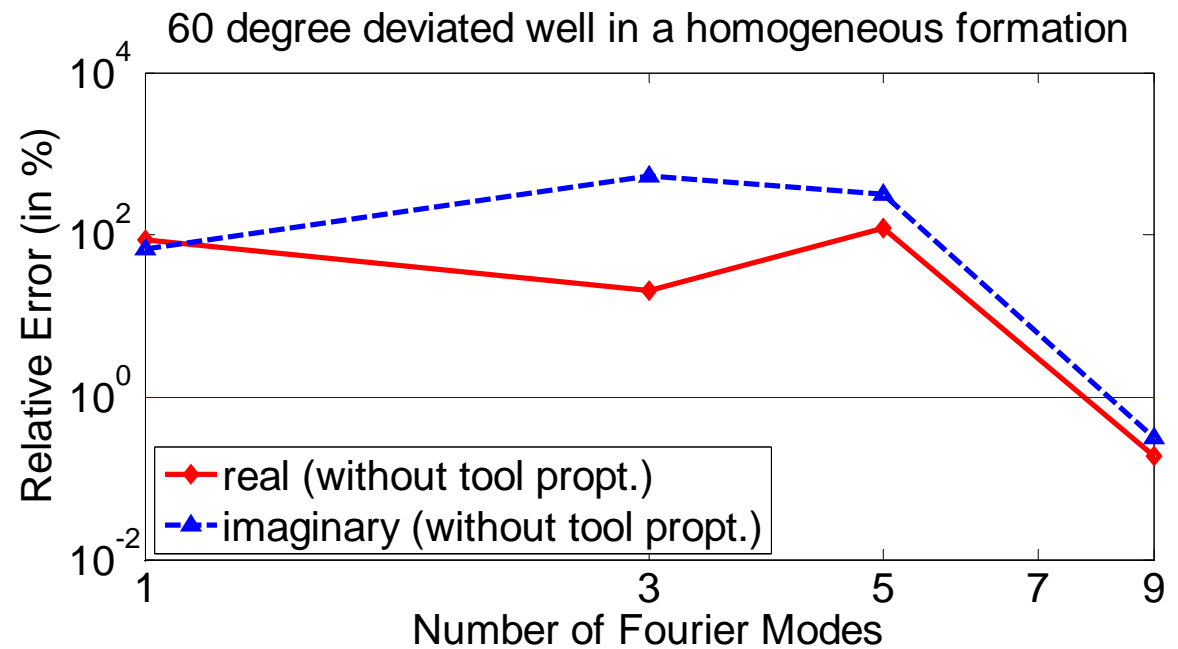


Verification of 3D Simulation (H_{xx})

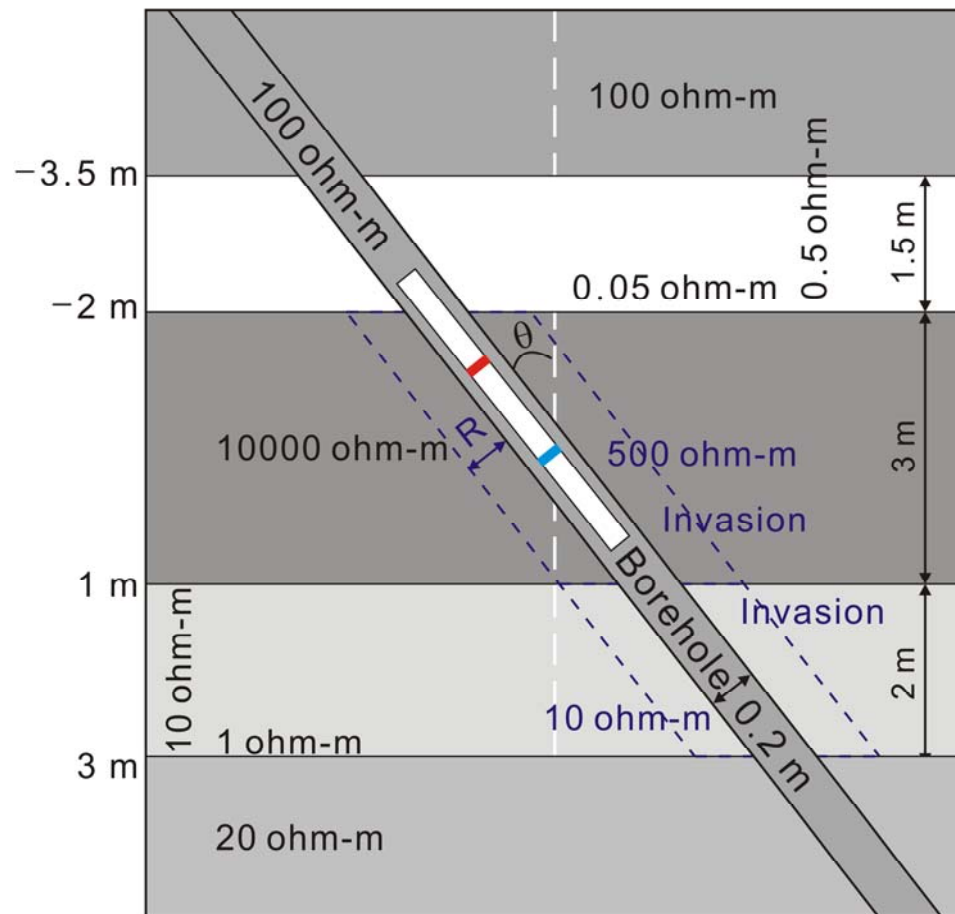
$\theta = 60$ degrees



Relative errors of tri-axial Induction solutions with respect to the solution for the vertical well



Model for Numerical Experiments



Five layers: 100, 0.05, 10000, 1 and 20 ohm-m from top to bottom

**Borehole: 0.1 m in radius
100 ohm-m in resistivity**

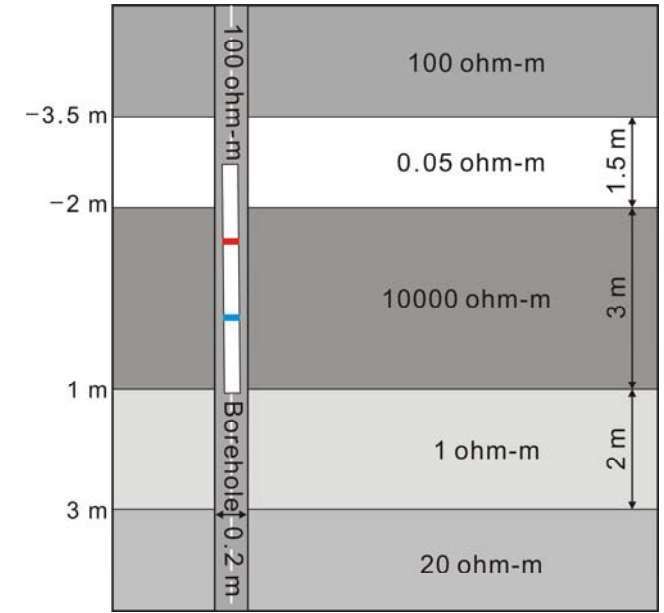
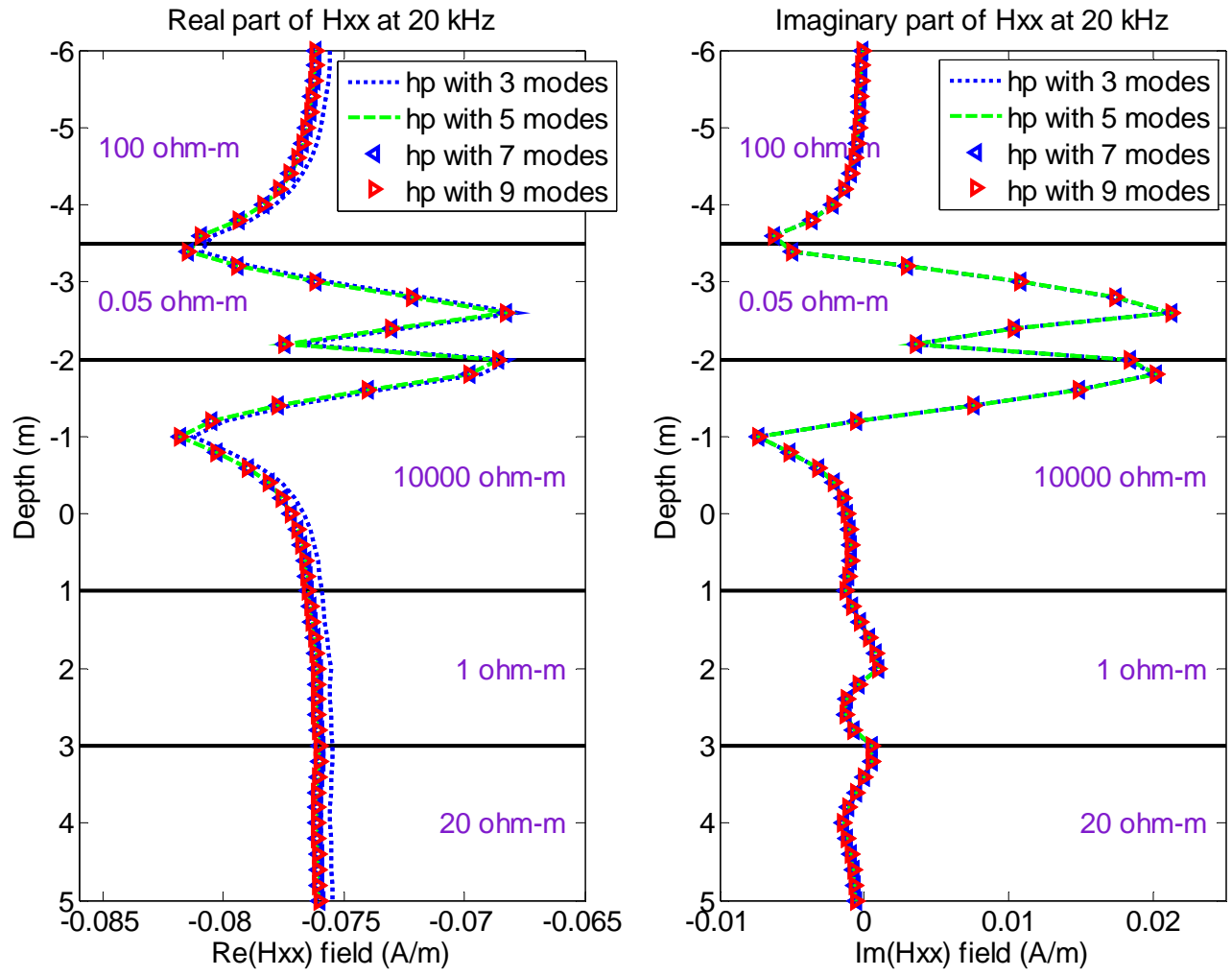
Invasion in the third and fourth layers

Anisotropy in the second and fourth layers

$\theta = 0, 30$ and 60 degrees



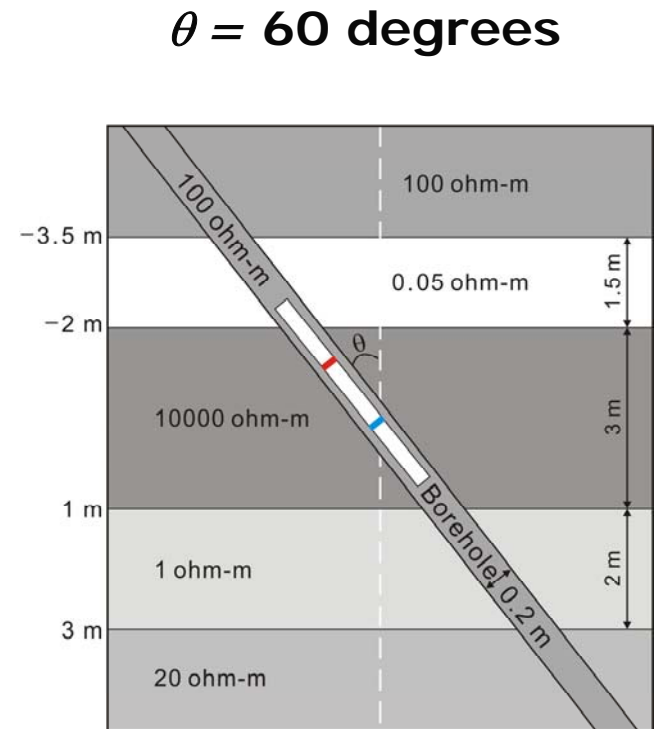
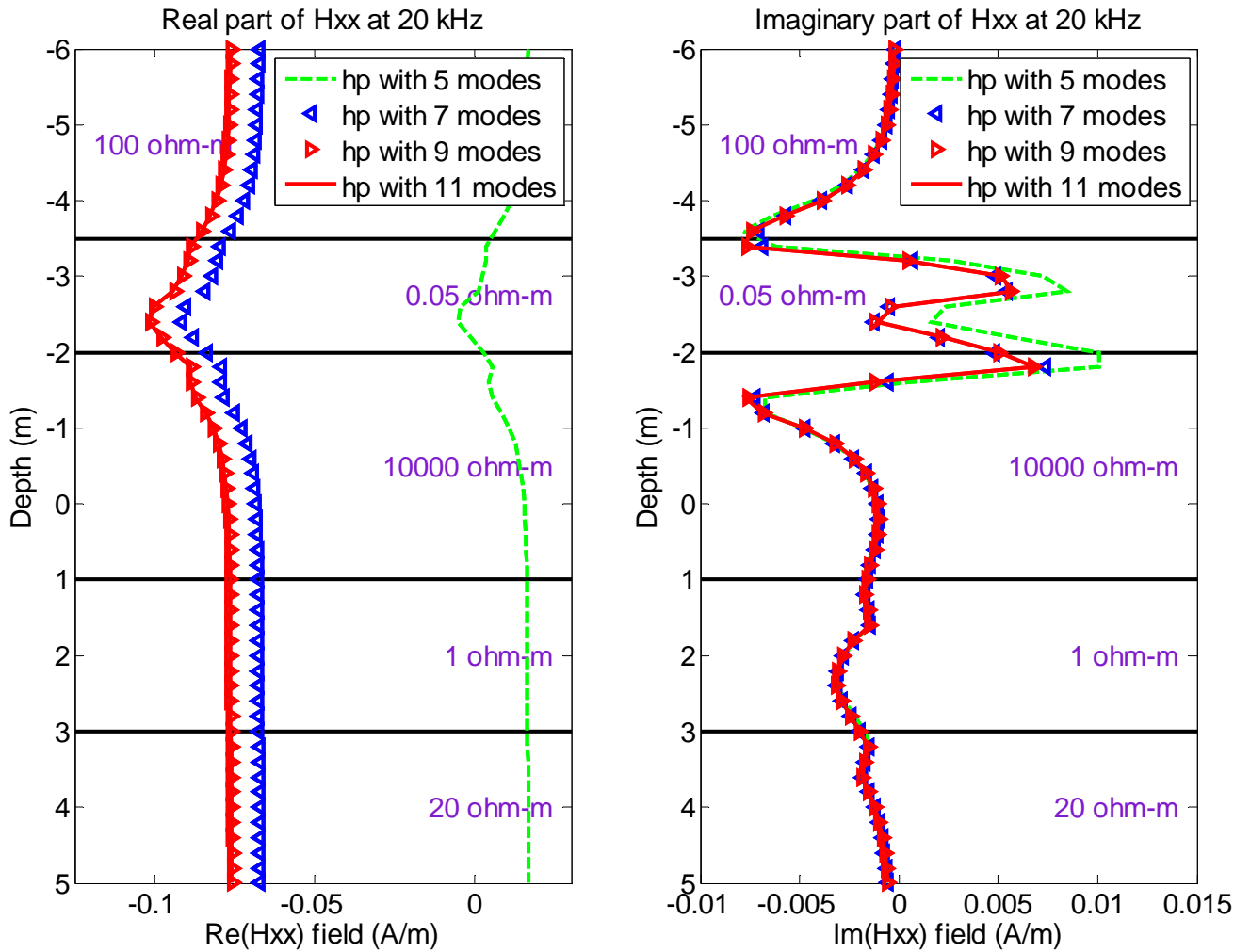
Convergence History of H_{xx} in Vertical Well



Converged solutions with 5 Fourier modes



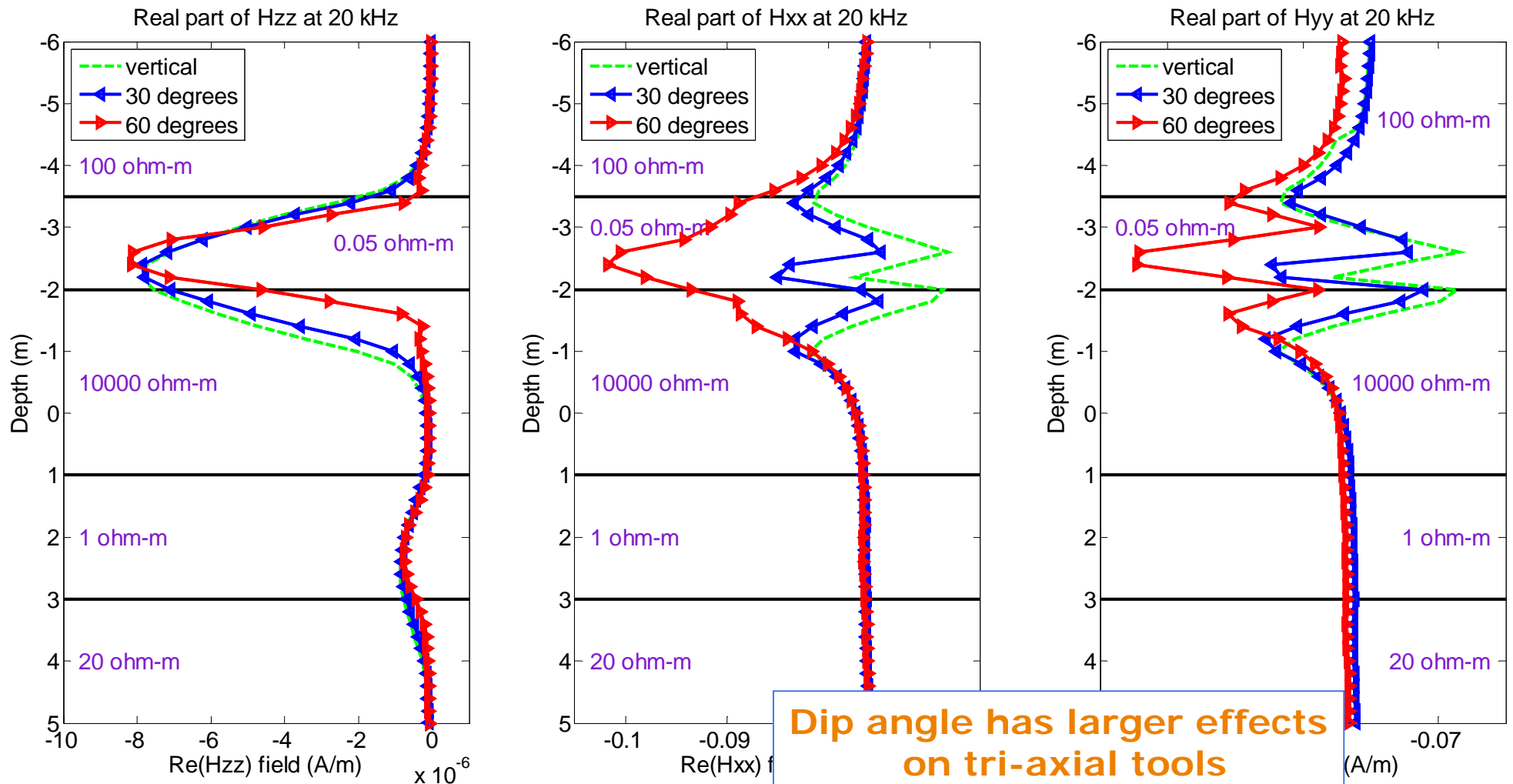
Convergence History of H_{xx} in Deviated Well



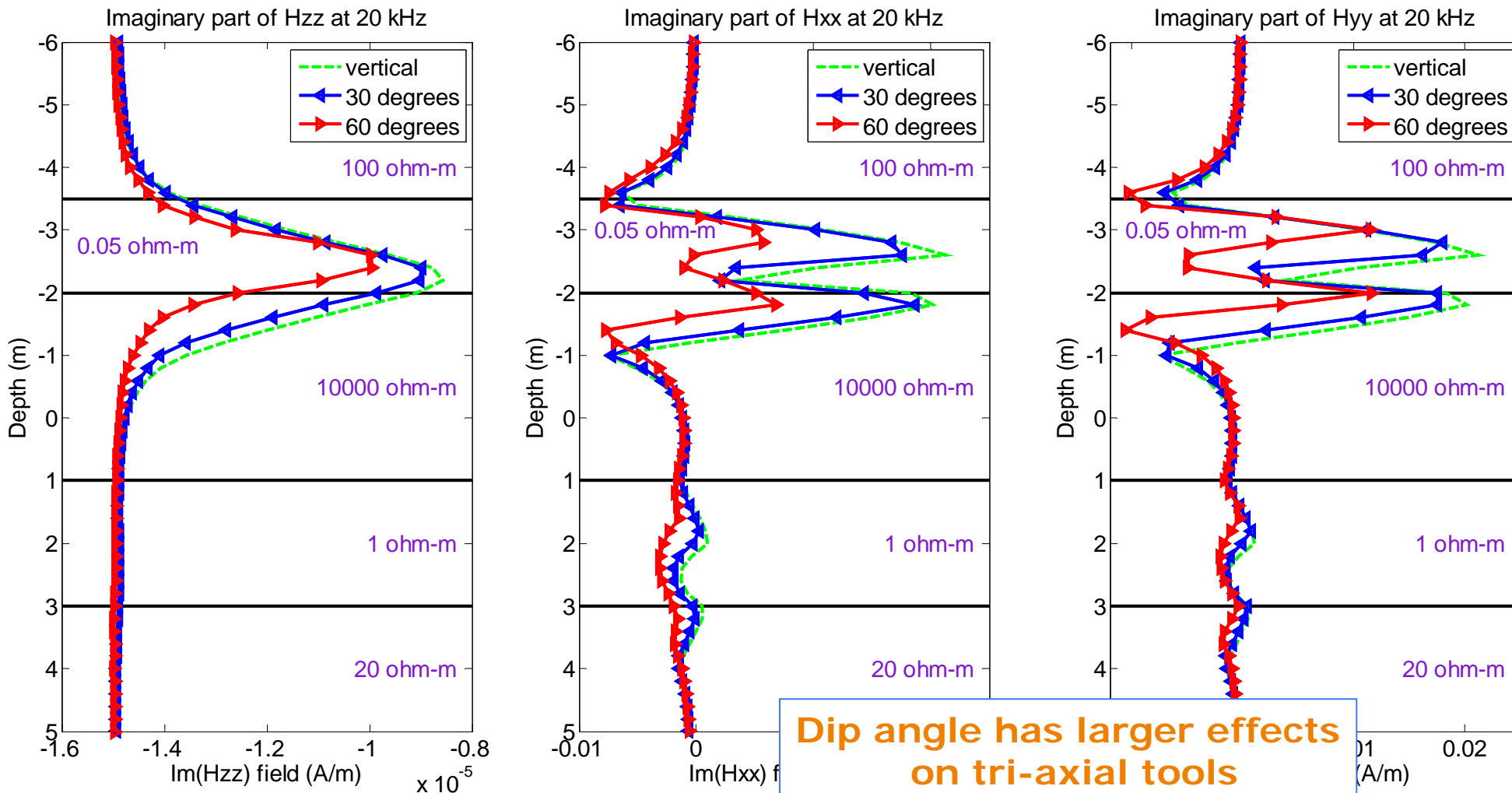
Converged solutions with 9 Fourier modes



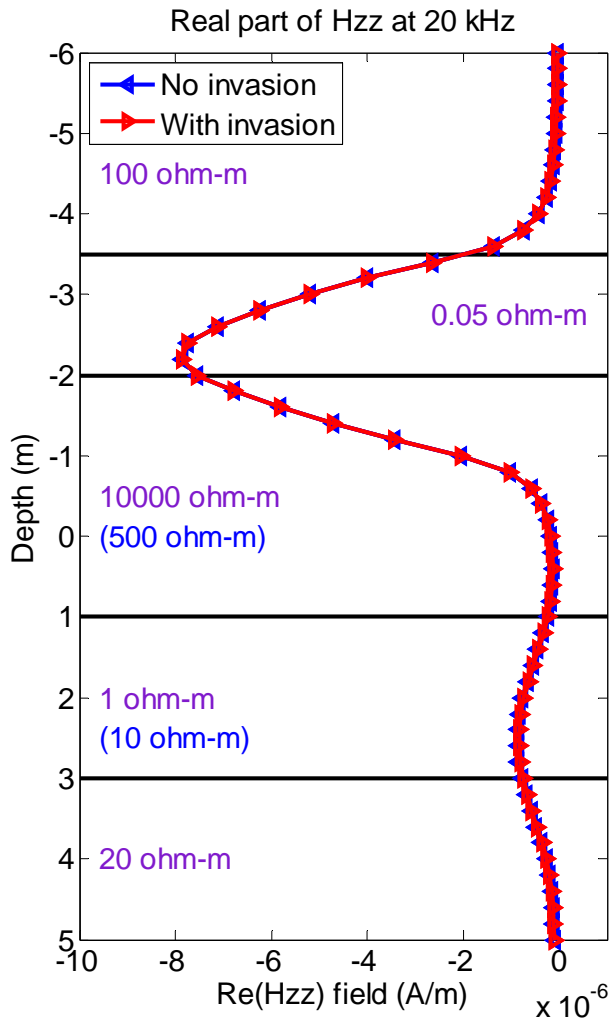
Deviated Wells (0, 30 & 60 degrees)



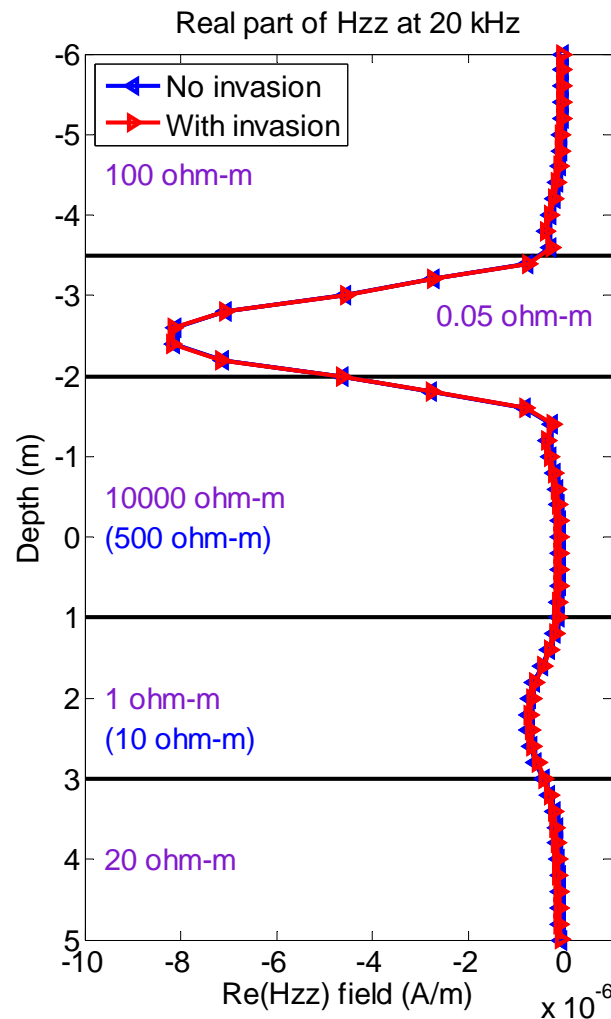
Deviated Wells (0, 30 & 60 degrees)



H_{zz} in Deviated Wells with Invasion (Re.)

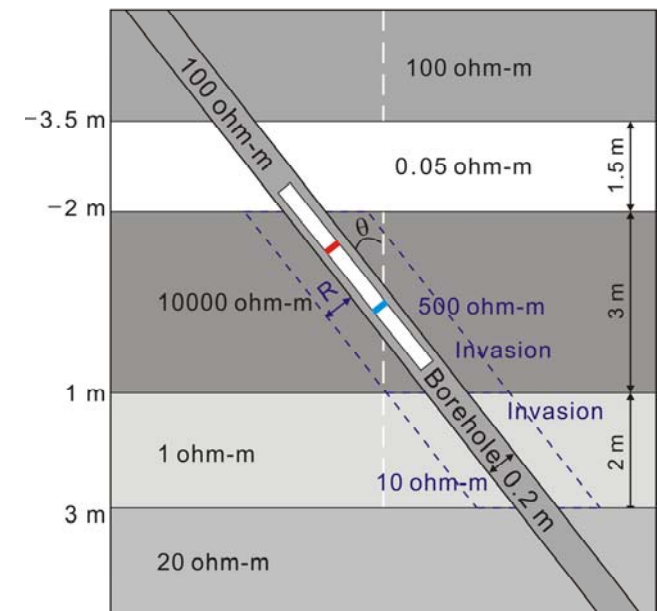


vertical

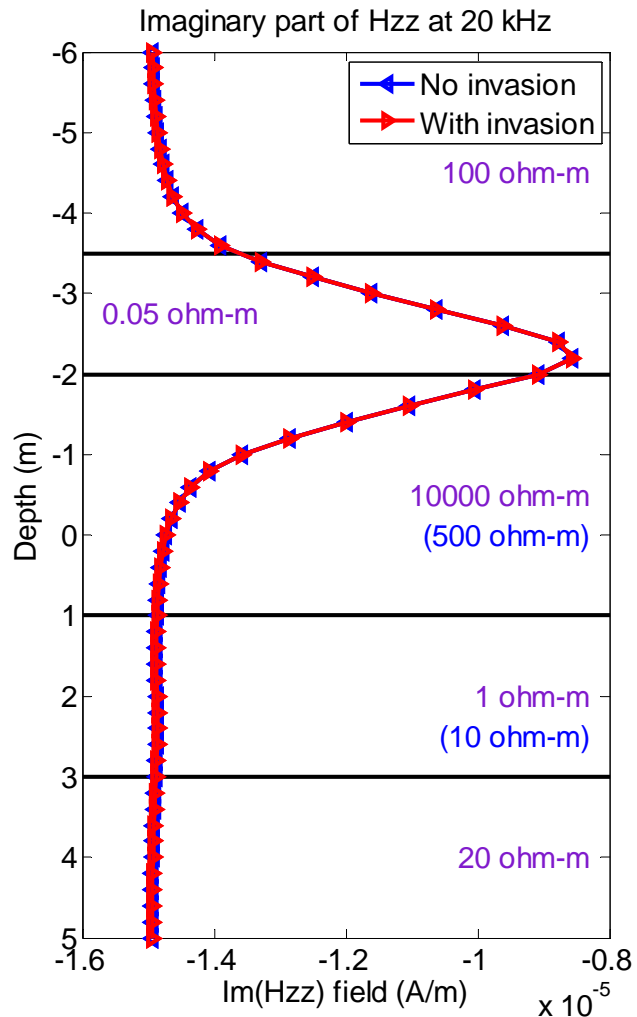


60 degrees

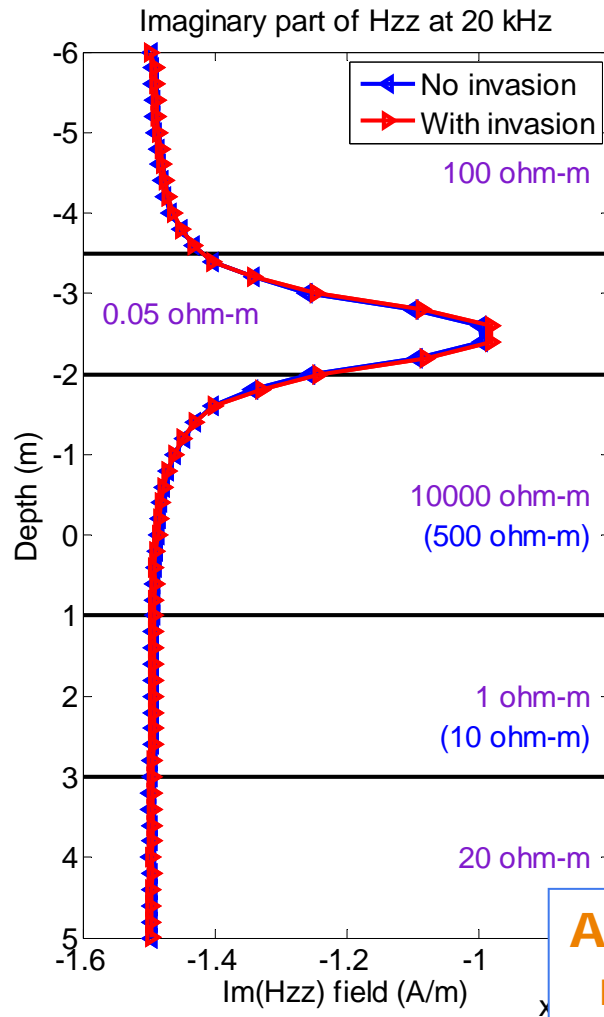
Shallow invasion with $R = 0.1$ m



H_{zz} in Deviated Wells with Invasion (Im.)

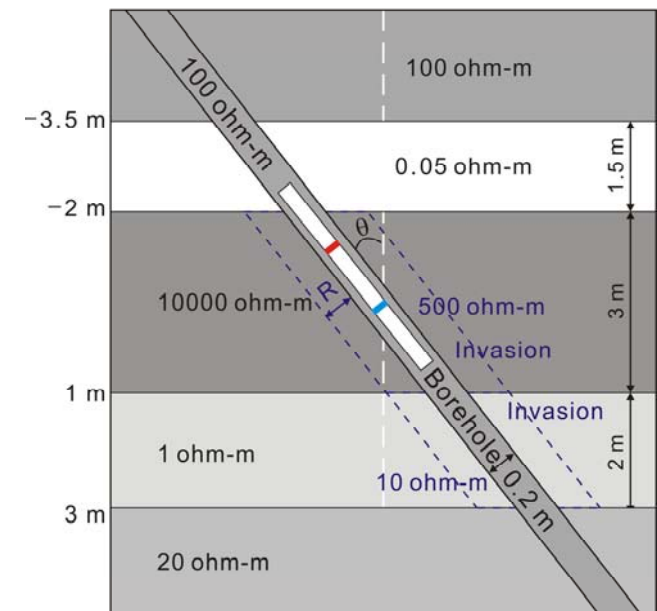


vertical



60 degrees

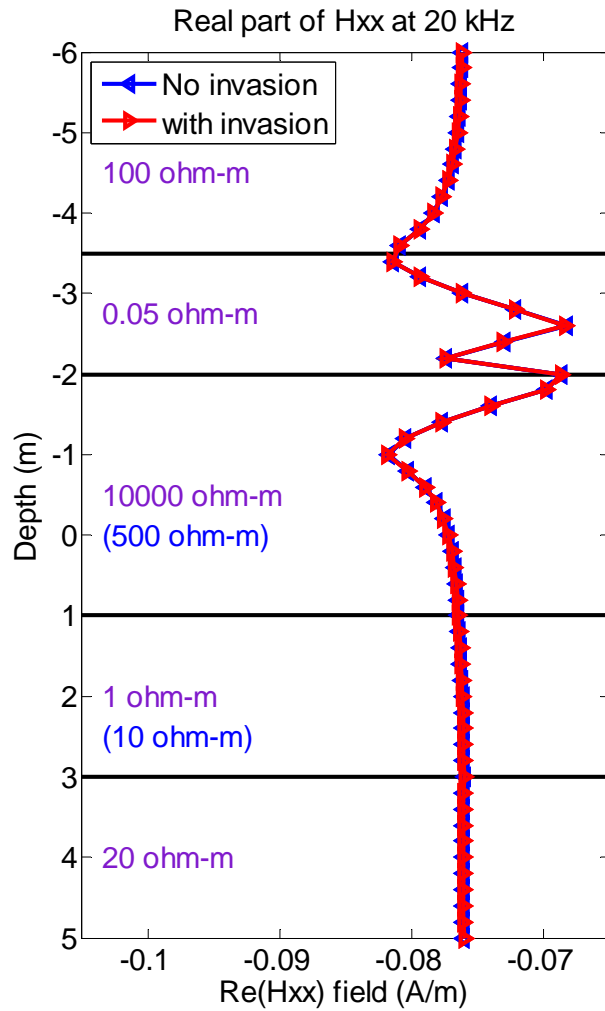
Shallow invasion with $R = 0.1$ m



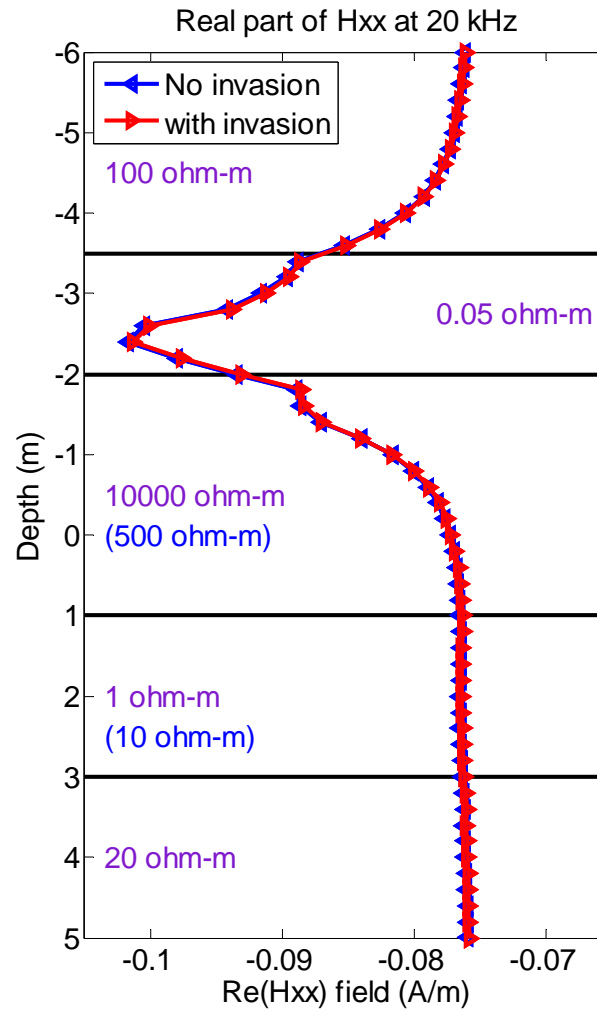
Almost no effects of invasion regardless of the dip angle



H_{xx} in Deviated Wells with Invasion (Re.)

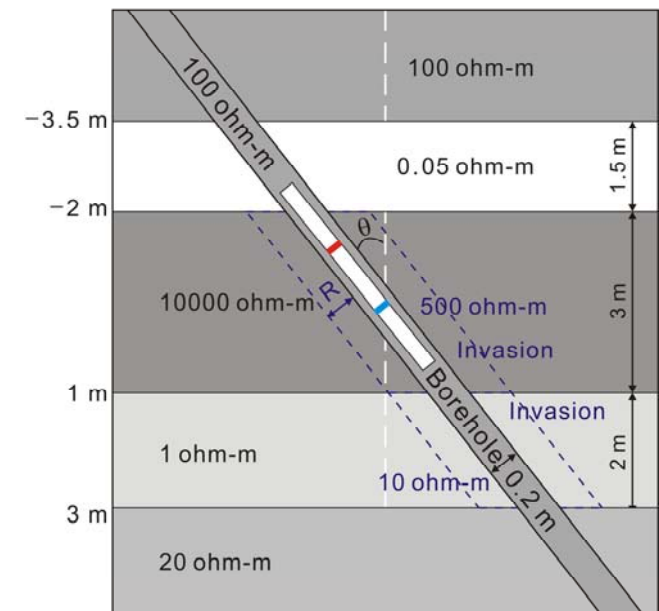


vertical

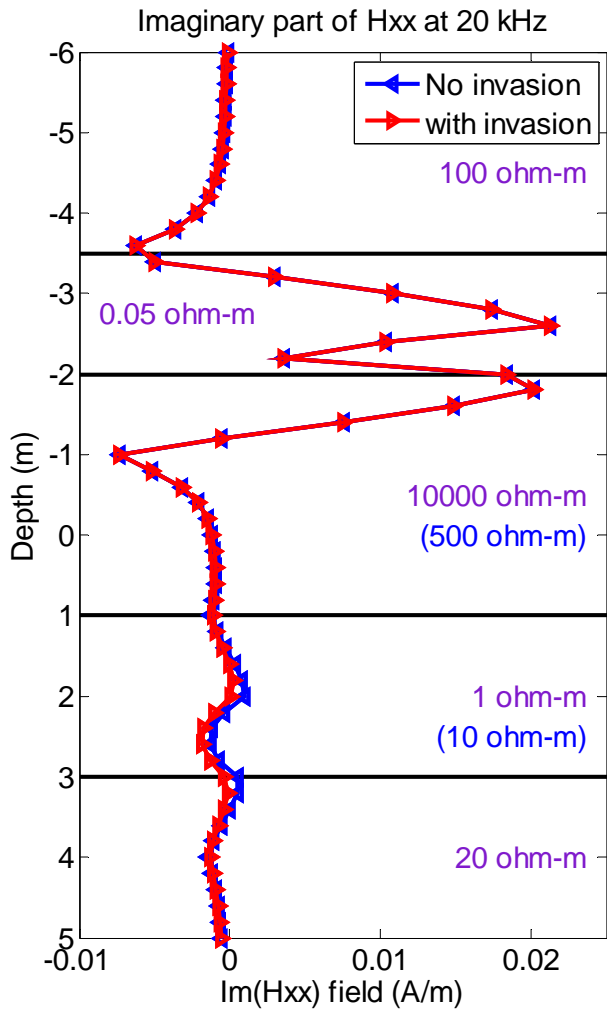


60 degrees

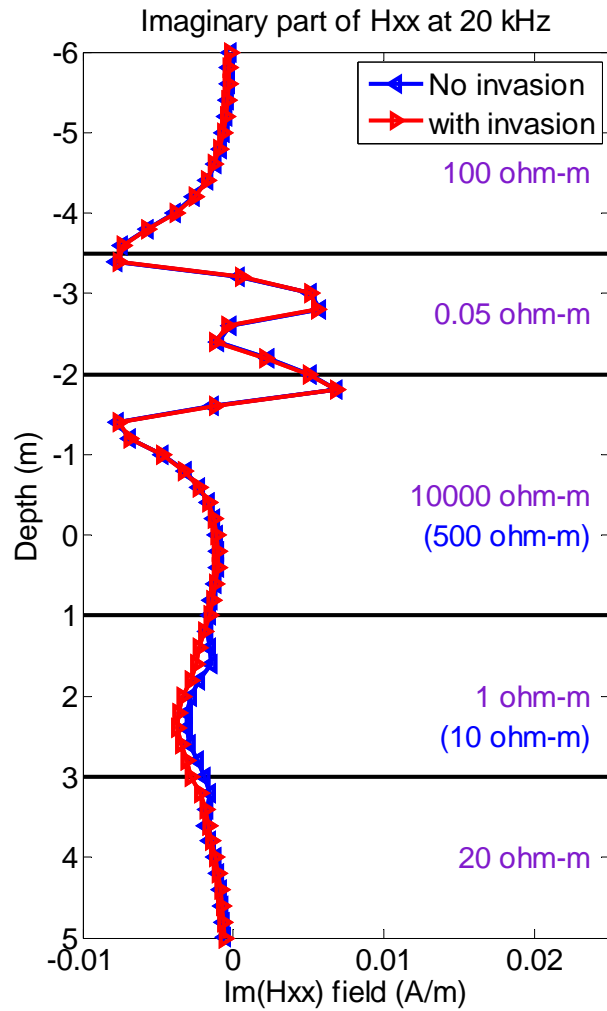
Shallow invasion with $R = 0.1$ m



H_{xx} in Deviated Wells with Invasion (Im.)

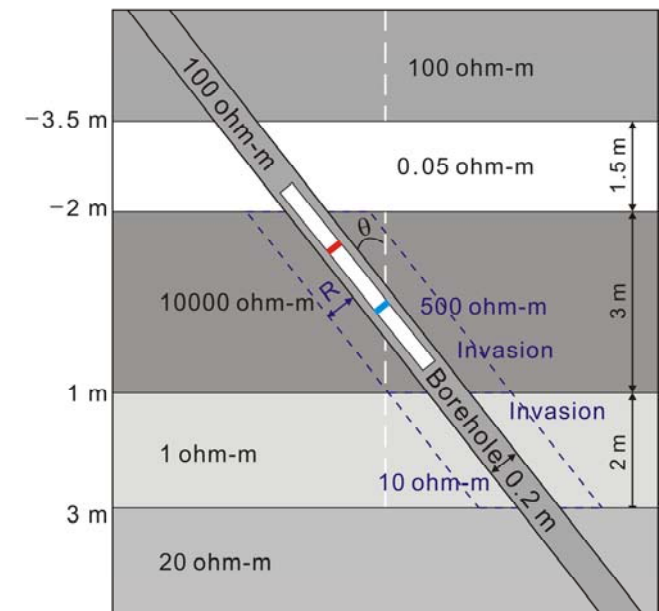


vertical



60 degrees

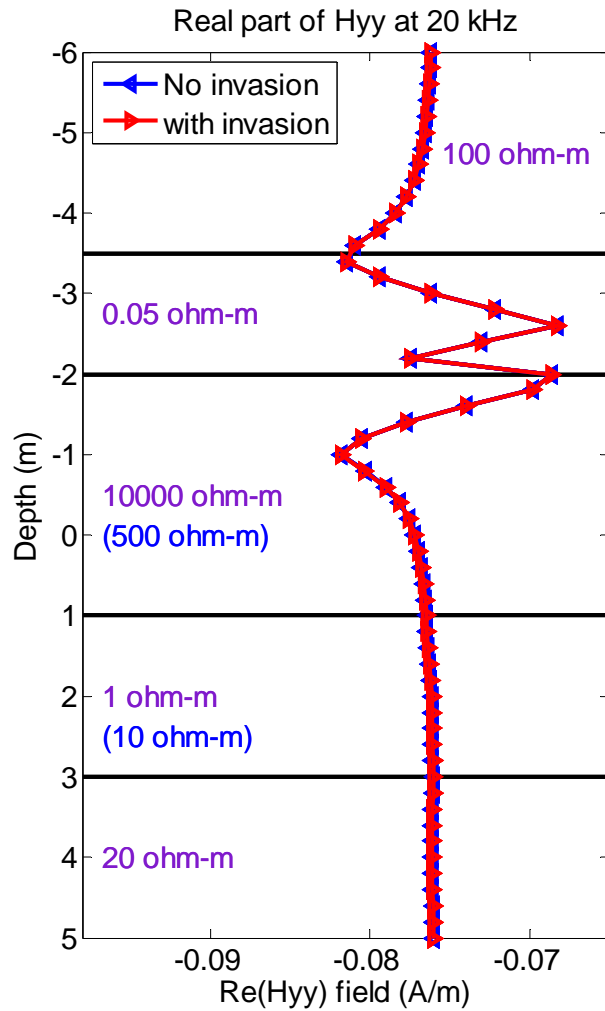
Shallow invasion with $R = 0.1$ m



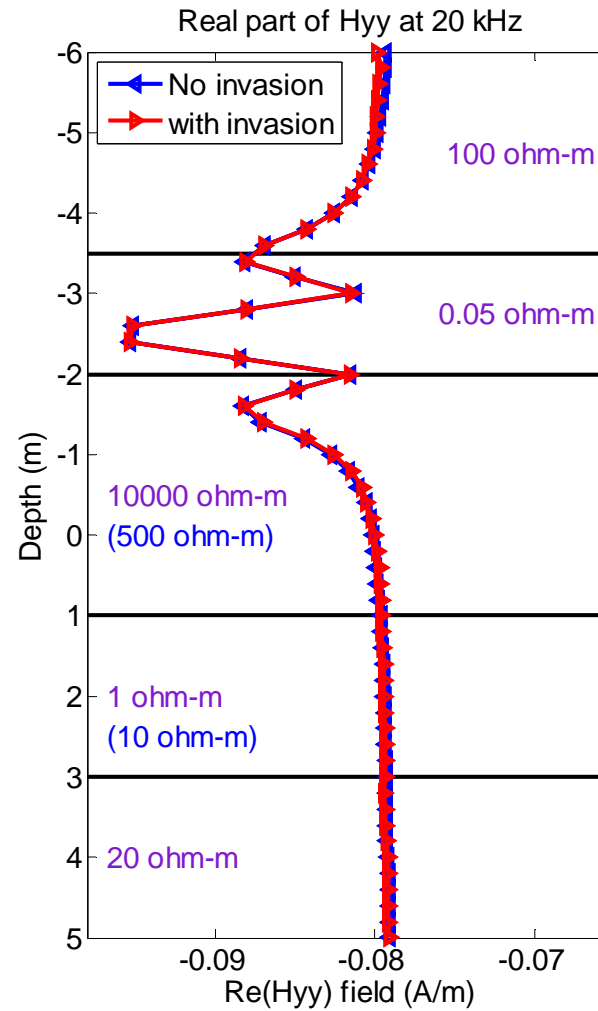
Small effects of invasion



H_{yy} in Deviated Wells with Invasion (Re.)

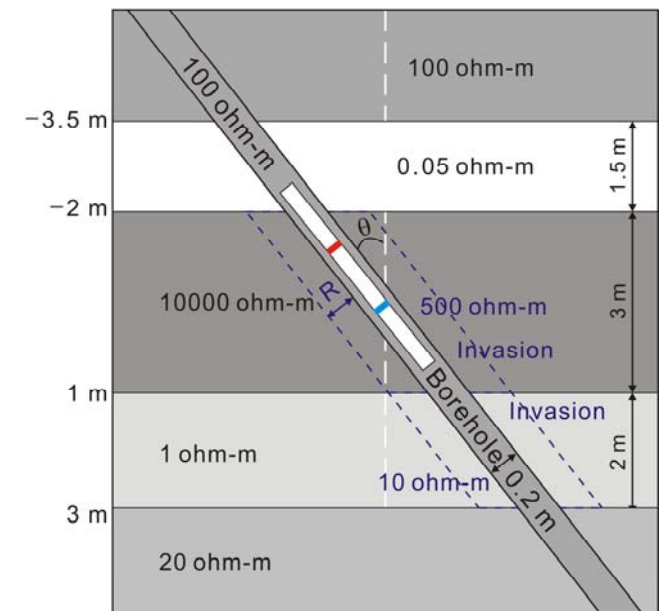


vertical

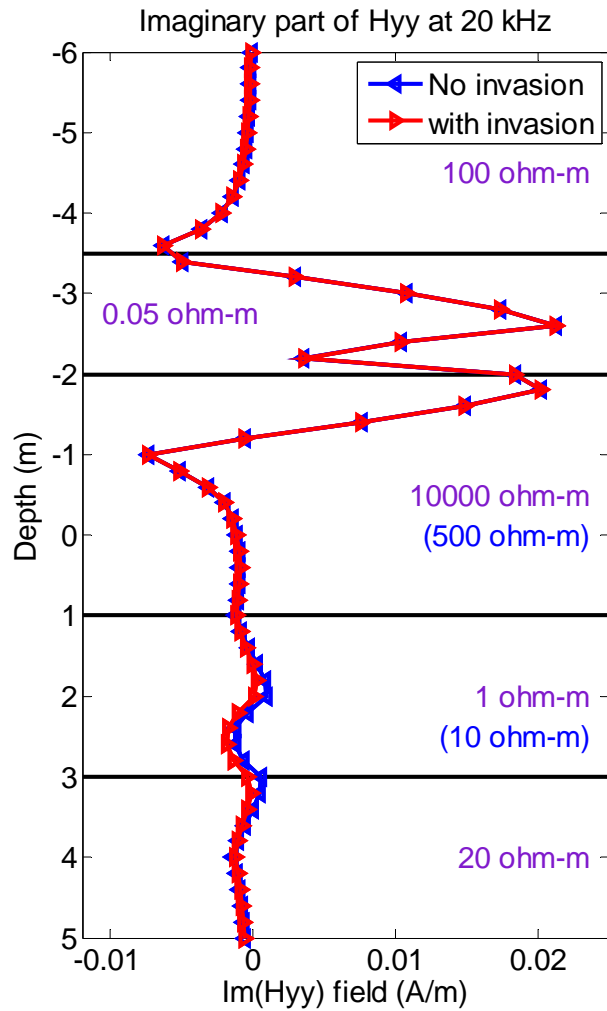


60 degrees

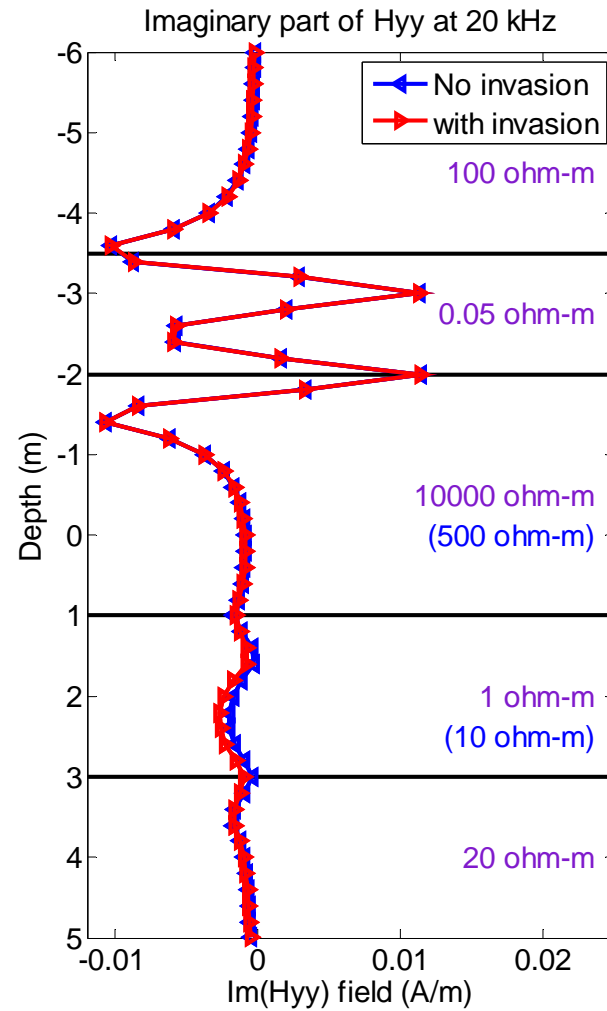
Shallow invasion with $R = 0.1$ m



H_{yy} in Deviated Wells with Invasion (Im.)

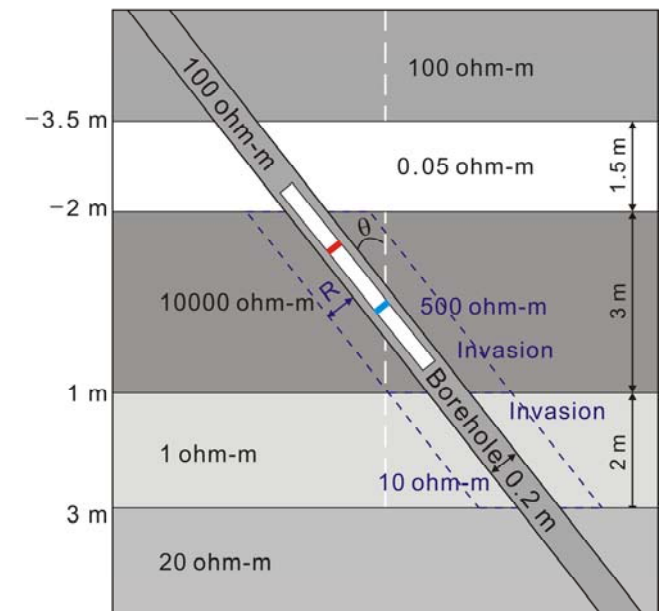


vertical



60 degrees

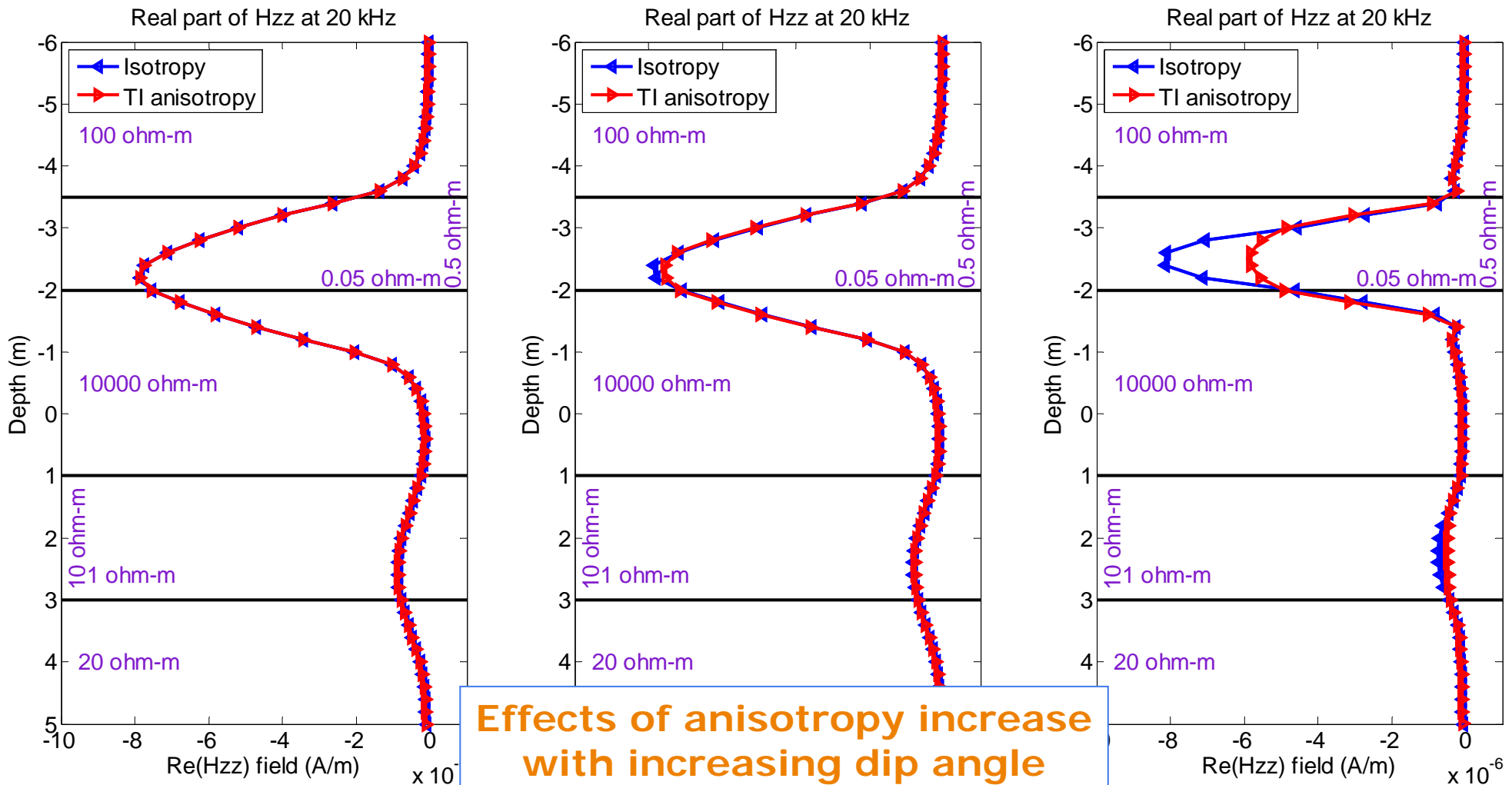
Shallow invasion with $R = 0.1$ m



Small effects of invasion



H_{zz} in Deviated Wells with Anisotropy (Re.)



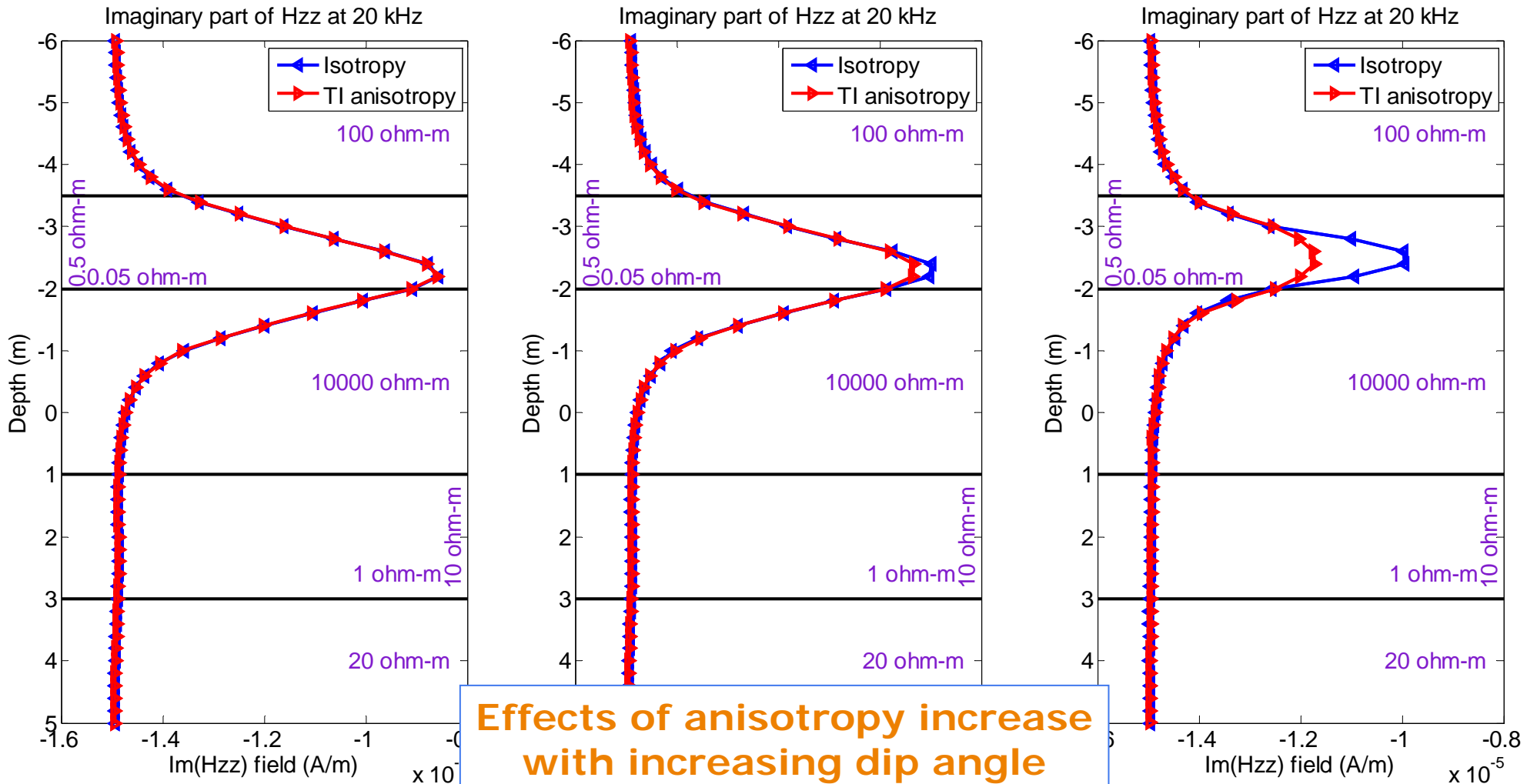
vertical

30 degrees

60 degrees



H_{zz} in Deviated Wells with Anisotropy (Im.)



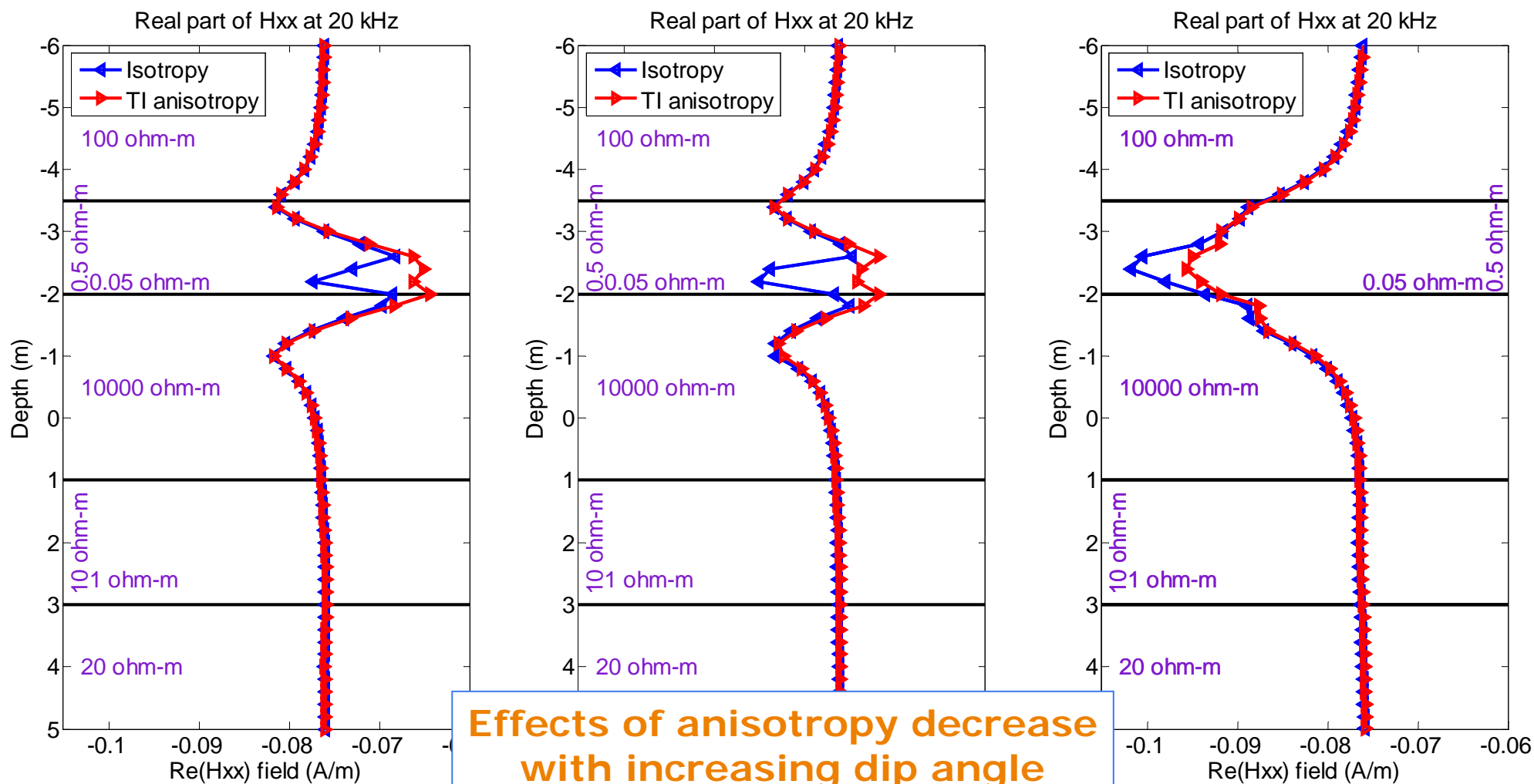
vertical

30 degrees

60 degrees



H_{XX} in Deviated Wells with Anisotropy (Re.)



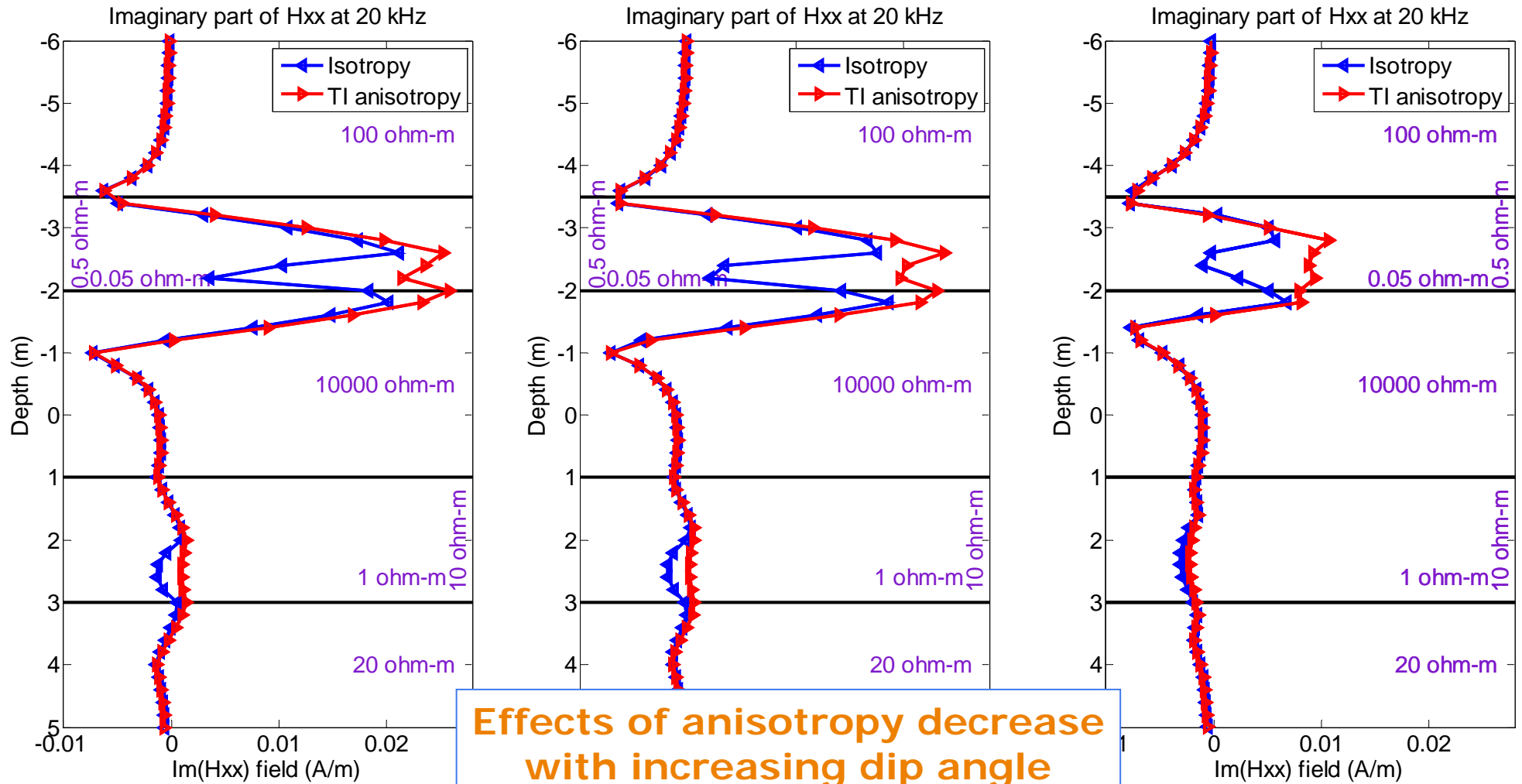
vertical

30 degrees

60 degrees



H_{XX} in Deviated Wells with Anisotropy (Im.)



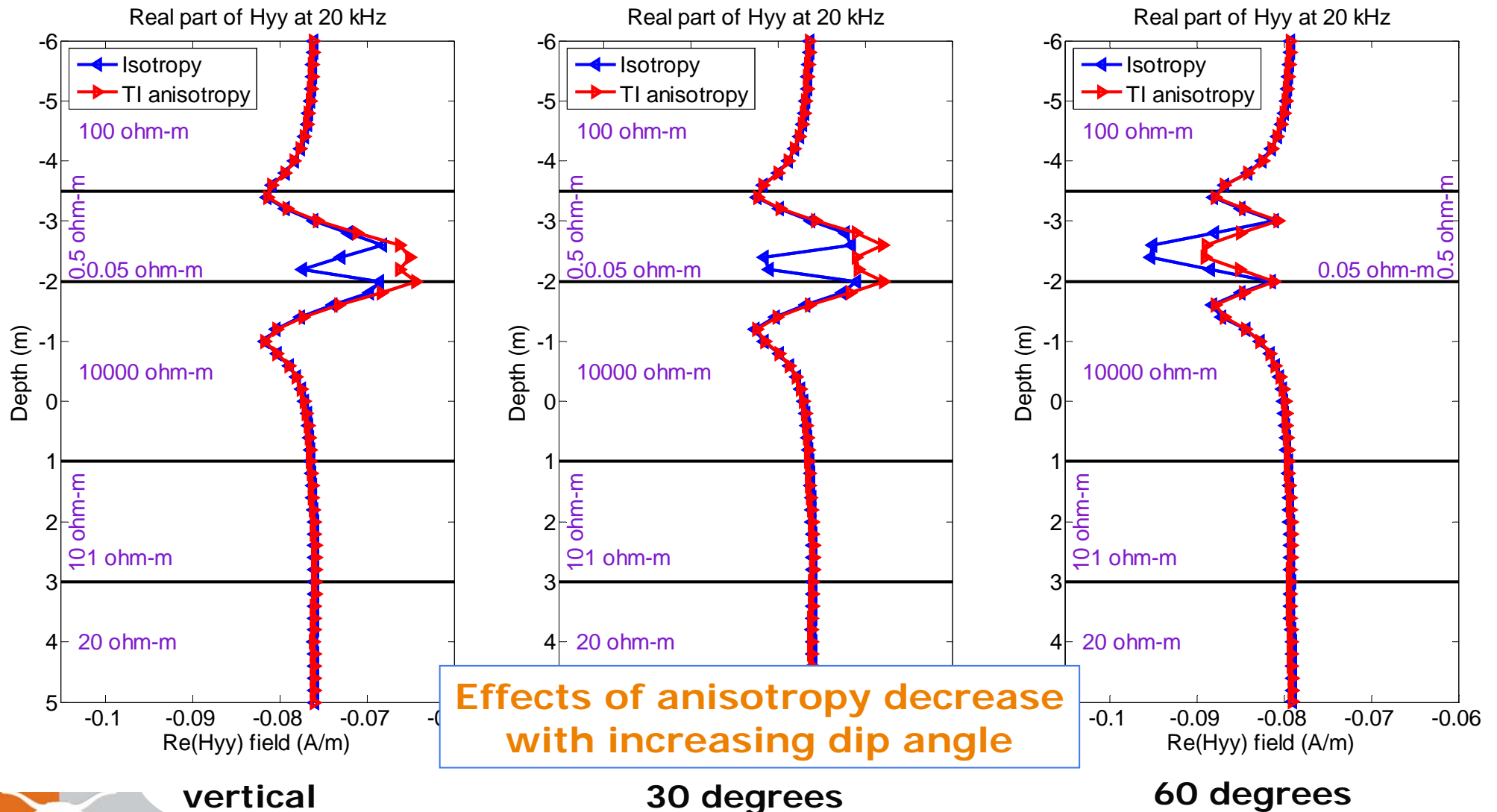
vertical

30 degrees

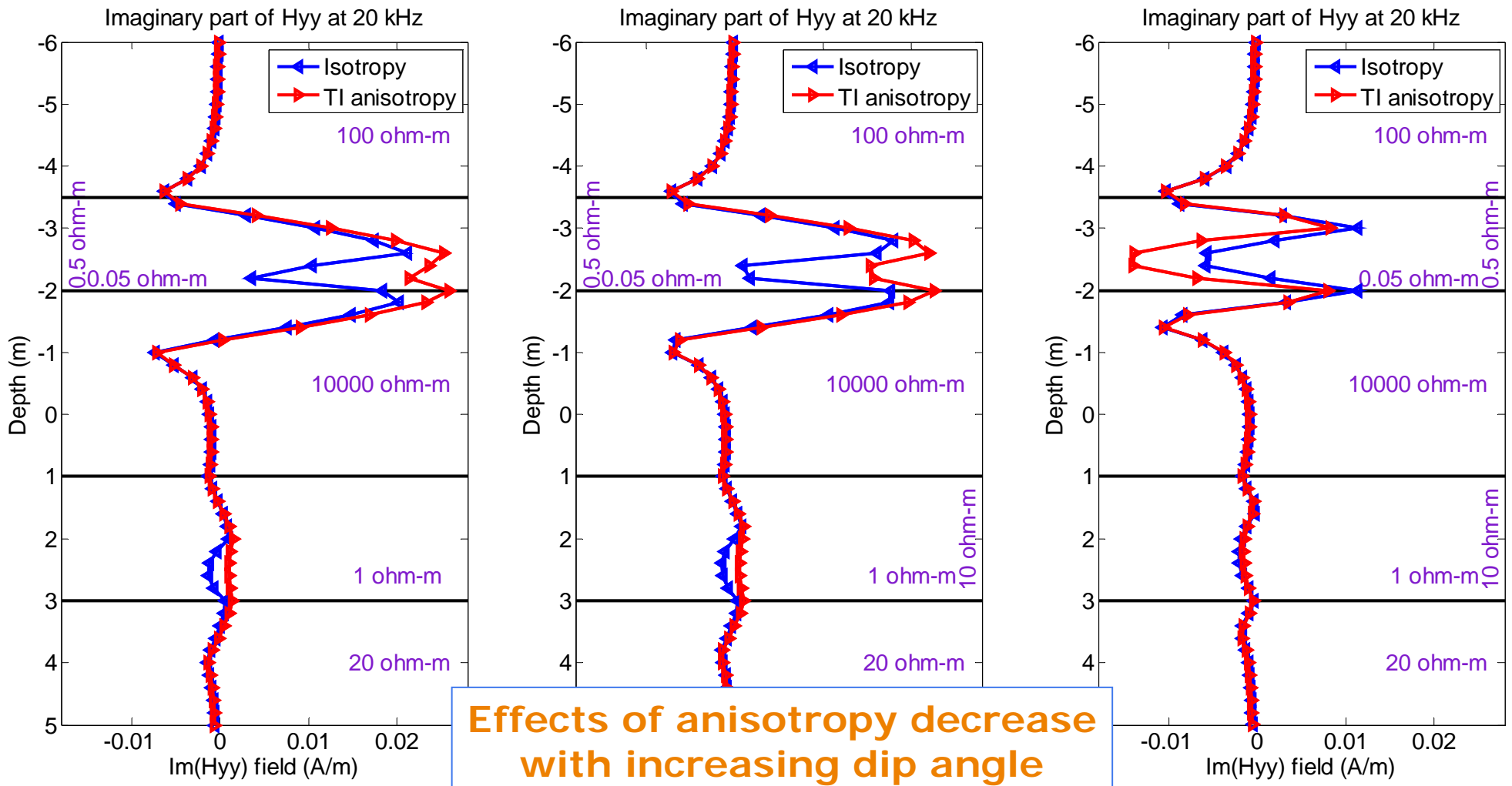
60 degrees



H_{yy} in Deviated Wells with Anisotropy (Re.)



H_{yy} in Deviated Wells with Anisotropy (Im.)



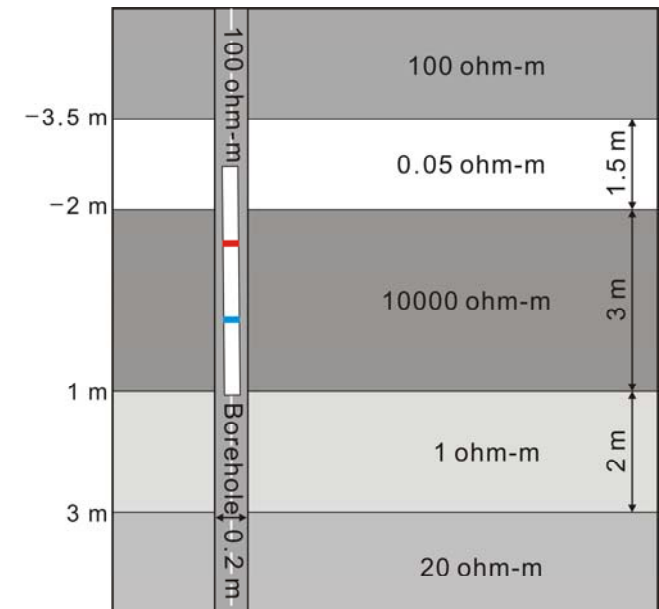
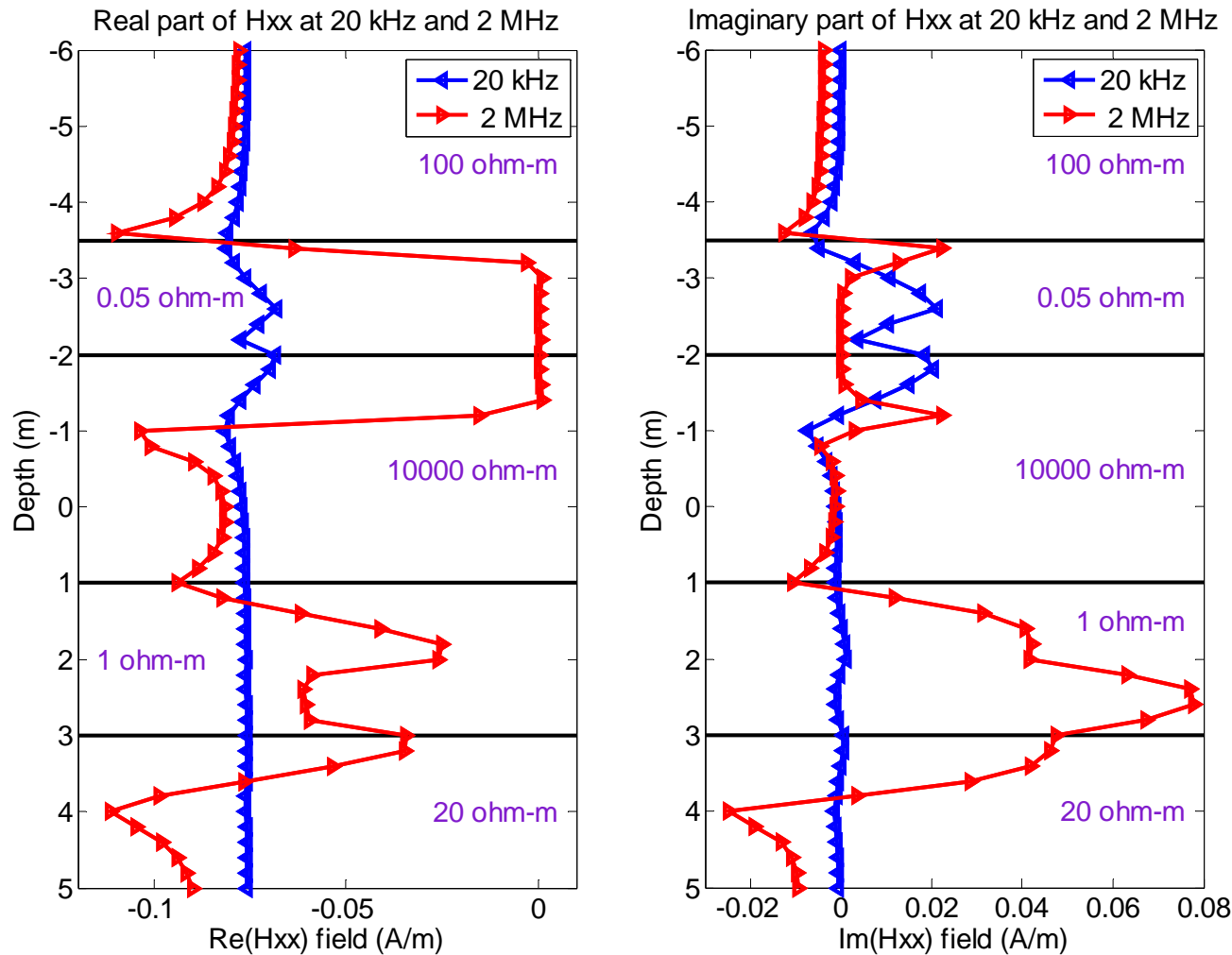
vertical

30 degrees

60 degrees



H_{xx} at 20 KHz and 2 MHz in Vertical Well



**Larger variations at 2 MHz
than at 20 kHz**



Conclusions

- We successfully simulated 3D tri-axial induction measurements by combining the use of a Fourier series expansion in a non-orthogonal system of coordinates with a 2D high-order, self-adaptive *hp* finite-element method.
- Dip angle effects on tri-axial tools are larger than on more traditional induction logging instruments.
- Anisotropy effects on H_{xx} and H_{yy} decrease with increasing dip angle, while those on H_{zz} increase.
- H_{xx} at 20 kHz exhibits smaller variations than at 2 MHz.



Acknowledgements

Sponsors of UT Austin's consortium on Formation Evaluation:



أرامكو السعودية
Saudi Aramco



ConocoPhillips



Eni

ExxonMobil

HALLIBURTON



INSTITUTO MEXICANO DEL PETRÓLEO



Schlumberger



StatoilHydro

